Longitudinal transcriptomic analysis of altered pathways in a CHMP2Bintron5-based model of ALS-FTD

Robin Waegaert, Sylvie Dirrig-Grosch, Florian Parisot, Céline Keime, Alexandre Henriques, Jean-Philippe Loeffler, Frédérique René

Neurobiology of Disease 136 (2020) 104710

Contents lists available at ScienceDirect

Neurobiology of Disease

journal homepage: www.elsevier.com/locate/ynbdi

Longitudinal transcriptomic analysis of altered pathways in a CHMP2B^{intron5}-based model of ALS-FTD

Robin Waegaert[a], Sylvie Dirrig-Grosch[a], Florian Parisot[a], Céline Keime[b], Alexandre Henriques[a], Jean-Philippe Loeffler[a], Frédérique René[a,*]

[a] INSERM U1118 Mécanismes centraux et périphériques de la neurodégénérescence, Université de Strasbourg, 11 rue Humann, Strasbourg, France
[b] Institut de Génétique et de Biologie Moléculaire et Cellulaire, INSERM U1258, CNRS, UMR7104, Université de Strasbourg, 1 Rue Laurent Fries, 67400 Illkirch-Graffenstaden, France

ARTICLE INFO

Keywords:
Amyotrophic lateral sclerosis
Frontotemporal dementia
Transcriptomic analysis CHMP2B^{intron5}
SOD1^{G86R}
Mouse models
Inflammation
Lipid metabolism
Ion transporters

ABSTRACT

Amyotrophic lateral sclerosis and frontotemporal dementia are two neurodegenerative diseases with currently no cure. These two diseases share a clinical continuum with overlapping genetic causes. Mutations in the *CHMP2B* gene are found in patients with ALS, FTD and ALS-FTD. To highlight deregulated mechanisms occurring in ALS-FTD linked to the *CHMP2B* gene, we performed a whole transcriptomic study on lumbar spinal cord from CHMP2B^{intron5} mice, a model that develops progressive motor alterations associated with dementia symptoms reminiscent of both ALS and FTD. To gain insight into the transcriptomic changes taking place during disease progression this study was performed at three stages: asymptomatic, symptomatic and end stage. We showed that before appearance of motor symptoms, the major disrupted mechanisms were linked with the immune system/inflammatory response and lipid metabolism. These processes were progressively replaced by alterations of neuronal electric activity as motor symptoms appeared, alterations that could lead to motor neuron dysfunction.

To investigate overlapping alterations in gene expression between two ALS-causing genes, we then compared the transcriptome of symptomatic CHMP2B^{intron5} mice with the one of symptomatic SOD1^{G86R} mice and found the same families deregulated providing further insights into common underlying dysfunction of biological pathways, disrupted or disturbed in ALS.

Altogether, this study provides a database to explore potential new candidate genes involved in the CHMP2B^{intron5}-based pathogenesis of ALS, and provides molecular clues to further understand the functional consequences that diseased neurons expressing CHMP2B mutant may have on their neighbor cells.

1. Introduction

Amyotrophic lateral sclerosis (ALS), the most common adult-onset motor neuron disease, is characterized by the degeneration of motor neurons associated with progressive muscle denervation and atrophy leading to paralysis and death usually within 2–5 years following diagnosis (Hand and Rouleau, 2002). Frontotemporal dementia (FTD) is the second most common cause of dementia in people under the age of 65 years after Alzheimer's disease (Ratnavalli et al., 2002). It mainly affects anterior temporal and/or frontal lobes of the brain, causing progressive degeneration of the frontal and temporal cortical neurons and subsequent dementia (Pressman and Miller, 2014).

Although selective groups of neurons are primarily affected in each disease (Lillo and Hodges, 2009) increasing evidence suggests that ALS and FTD may fall into the same disease spectrum (Gascon and Gao, 2014; Ling et al., 2013). ALS and FTD share common pathophysiological features with overlapping genetic causes. Approximately 15–20% of ALS patients present with cognitive impairment reminiscent of FTD and approximately 15% of FTD patients develop ALS (Lillo and Hodges, 2009; Phukan et al., 2012). Therefore, ALS and FTD are now considered overlapping clinical syndromes with common causes. Understanding the common mechanisms and biochemical pathways driving the

Abbreviations: ALS, Amyotrophic Lateral Sclerosis; AS stage, asymptomatic stage; CHMP2B, Charged Multivesicular Body protein 2B; E stage, end stage; FC, fold change; FTD, FrontoTemporal Dementia; nTg, non-transgenic; PAF, platelet activating factor; ROS, reactive oxygen species; SLC, solute carrier family; SOD1, superoxide dismutase 1; S stage, symptomatic stage; Tg, transgenic

* Corresponding author at: INSERM U1118 Mécanismes centraux et périphériques de la neurodégénérescence, Université de Strasbourg, 11 rue Human, Bâtiment 3, 67000 Strasbourg, France.
E-mail address: frederique.rene@unistra.fr (F. René).

https://doi.org/10.1016/j.nbd.2019.104710
Received 5 February 2019; Received in revised form 28 October 2019; Accepted 8 December 2019
Available online 16 December 2019

neurodegenerative processes in these diseases is essential to delineate new therapeutic strategies that could be used for the diseases belonging to this continuum.

Among the genes associated with these two diseases, mutations in the *CHMP2B* (*Charged Multivesicular Body protein 2B*) gene, although rare, are found in patients with ALS (Parkinson et al., 2006; Cox et al., 2010; van Blitterswijk et al., 2012; Narain et al., 2018), FTD (Skibinski et al., 2005; van der Zee et al., 2008; Ghanim et al., 2010) and ALS-FTD (Parkinson et al., 2006) supporting the idea that ALS and FTD belong to a pathological continuum linking these two diseases.

CHMP2B is a member of the Charged Multivesicular Body Protein family. This protein contributes to the ESCRT-III complex (endosomal sorting complex required for transport III), which is involved in endocytic-lysosomal trafficking of proteins and autophagy (Urwin et al., 2009; Ghazi-Noori et al., 2012). From ongoing studies, multiple pathogenic processes have been proposed for CHMP2B mutants: disruption of *endo*-lysosomal trafficking, misregulation of transmembrane receptors, abnormal substrate degradation, down regulation of a brain-specific microRNA (Gascon et al., 2014) or abnormal dendritic spine morphology (Chassefeyre et al., 2015). However the precise mechanisms leading to disease pathogenesis and progression are still poorly understood. Indeed, ALS and FTD are complex non-cell autonomous multifactorial diseases where both neurons and glia play a critical role in disease progression (Hallmann et al., 2017; Pramatarova et al., 2001; Qian et al., 2017).

Transcriptomic analysis represents a powerful tool to analyze the complexity of disease pathobiology, to shed light on the cascade of events underlying the disease and to identify novel gene targets for therapeutic intervention. Gene expression studies performed on mutant SOD1 ALS mouse models or on tissues from sporadic ALS patients have provided invaluable insights into the molecular mechanisms involved in ALS, supporting a “multiple-hit” hypothesis of neurodegeneration. In this regard, a number of converging pathogenic mechanisms are known, including oxidative damage, defective protein misfolding, mitochondrial degeneration, impaired axonal transport, neurotrophic factor deficits, apoptosis, aberrant RNA/DNA regulation, and neuroinflammation (Krokidis and Vlamos, 2018). However, little is known about the transcriptional changes associated with *CHMP2B* mutations. To date, 12 mutations have been described in ALS (7 mutations), ALS-FTD (1 mutation) and FTD (4 mutations) patients. The *CHMP2B* mutations are disseminated throughout the sequence, irrespective of the considered pathology (Krasniak and Ahmad, 2016). In 2010, Cox and collaborators analyzed the transcriptome of spinal motor neurons from 4 ALS patients bearing different *CHMP2B* mutations (c311 C > A; c85 A > G; c618 A > C) located in exons 2, 3 and 6. They found a distinct gene expression signature with an alteration of pathways related to ER and Golgi function, vesicular transport, mTOR signaling and autophagy, MAPK and calcium signaling, axon guidance, cell cycle and apoptosis, and regulation of actin cytoskeleton. More recently Zhang and collaborators performed a RNAseq analysis on forebrain-type cortical neurons derived from human induced pluripotent stem cells obtained from patients carrying the 31449G > C mutation (Zhang et al., 2017). This mutation generates a G to C transition in the 5′ acceptor splice site of exon 6, producing two aberrant transcripts: CHMP2B ^{intron5} and CHMP2B$^{\Delta 10}$ leading to a troncation of 36 amino acids at the C-terminal part of the protein. Interestingly, this deleted region contains point mutation sites found in ALS (Cox et al., 2010) and FTD (Ghanim et al., 2010) patients, suggesting a common contribution of this region to both pathologies. In addition to misregulation of genes related to endolysosomal pathway, mitochondria and oxidative stress, this study brought to light an alteration of genes involved in iron homeostasis that may trigger mitochondrial alterations, ROS production and neuronal damages. Although giving important informations about the mechanisms activated by CHMP2B mutants, these two studies present some limitations. Indeed, in both cases, the alteration of genomic profiles found are cell-type specific. Thus the obtained results can neither reflect the global changes at a whole tissue level with complex cell-cell interactions, nor the changes of genomic profiles associated with disease progression.

We have previously shown in transgenic mice that CHMP2B^{intron5} mutant specifically expressed in neurons using the Thy1.2 promoter triggers a progressive age-dependent motor phenotype associated with behavioral changes that recapitulate ALS and FTD disorders (Vernay et al., 2016). In an attempt to better understand the mechanisms linking CHMP2B^{intron5} to ALS in this model and to investigate the impact of CHMP2B^{intron5} neuronal expression in a global context we performed a transcriptomic analysis based on RNA-sequencing on lumbar spinal cord of this transgenic CHMP2B^{intron5} mouse model. To gain access to the changes associated with disease progression, gene profiling was performed at three time-points corresponding to asymptomatic, symptomatic and end stage of the disease. In a second step, in an attempt to investigate overlapping alterations in gene expression between two ALS-causing genes, we compared the transcriptome of symptomatic CHMP2B^{intron5} mice with the one of symptomatic SOD1^{G86R} mice previously published by our laboratory (Henriques et al., 2017a, 2017b).

2. Material and methods

2.1. Ethics statement

All animal experimentations were performed in accordance with institutional and national guidelines, and approved by the local ethical committee from Strasbourg University (CREMEAS) and the ministry of higher education and research under numbers; AL/25/32/02/13, AL/51/58/02/13, APAFIS#2255, APAFIS#9494 in accordance with European regulations (Directive 2010/63/EU).

2.2. Animals

Homozygous CHMP2B^{intron5} transgenic mice overexpressing the human CHMP2B^{intron5} mutant under the Thy1.2 promoter were obtained by breeding hemizygous mice carrying 6 copies of the transgene (mixed FVB/N-DBA/2-C57BL/6 background) and were genotyped as previously described (Vernay et al., 2016). Male homozygous mice carrying 12 copies of the transgene (Tg) were used in this study and compared with control non-transgenic (nTg) littermates. Transgenic mice overexpressing murine SOD1 with the G86R mutation were genotyped as previously described (Ripps et al., 1995).

Mice were group-housed (2–5 per cage) in the animal facility of the medicine faculty of Strasbourg University, in a temperature- and humidity-controlled environment at 22 ± 1 °C under a 12-h light/dark cycle with unrestricted access to regular A04 rodent chow and water.

CHMP2B^{Intron5} mice were studied at three pre-defined stages of disease progression: at 1.5 month of age, an asymptomatic (AS) stage when motor symptoms are absent; at 6 months of age corresponding to the symptomatic (S) stage of the disease when mice develop signs of hindlimb weakness; and at 10–12 months of age corresponding to the end (E) stage of the disease when mice display hindlimb paralysis or loss of the righting reflex. SOD1^{G86R} mice were studied at 90 days corresponding to the S stage of the disease when mice develop signs of hindlimb weakness. At the selected time points, mice were sacrificed by lethal injection of pentobarbital (120 mg/kg IP). Tissues were carefully dissected, snap-frozen in liquid nitrogen and stored at −80° or fixed by immersion in paraformaldehyde 4% in 0.1 M phosphate buffer pH 7.4 until use. Detailed protocols for histology are given in supplementary material.

2.3. RNA extraction

Total RNA was prepared following standard protocols. Briefly, each frozen sample was placed into a tube containing a 5-mm stainless steel bead. Working on ice, 1 mL Trizol reagent (Invitrogen, Groningen, The

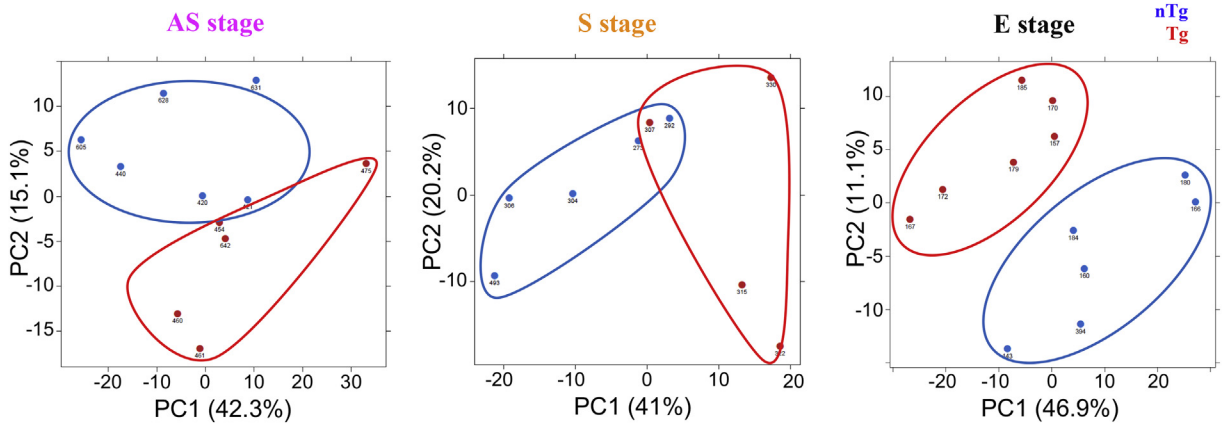

Fig. 1. Global transcriptomic signature in spinal cord. Gene expression profiles of CHMP2B^{intron5} mice (Tg) were compared to non transgenic littermates (nTg) at three stages of the disease: asymptomatic (AS), symptomatic (S) and end (E) stages. Principal Component Analyses were computed on regularized logarithm transformed data for each stage using all genes expressed in at least one represented sample. The first factorial planes are represented on these figures and the variability explained by each axe is provided into brackets. Tg mice are plotted in red and nTg mice are plotted in blue. (For interpretation of the references to colour in this figure legend, the reader is referred to the web version of this article.)

Netherlands) was added, and homogenization was performed twice in a TissueLyser (Qiagen) at 30 Hz for 3 min. Samples for RNA-sequencing analysis were then processed using the RNeasy Mini Kit (Qiagen, 74,104) according to manufacturer instructions. For RT-qPCR, RNA was extracted with chloroform/isopropyl alcohol/ethanol technic. Samples were stored at −80 °C until use.

2.4. RNA-sequencing

RNA-sequencing was performed by the GenomEast platform. Libraries were generated from 500 ng of total RNA using TruSeq Stranded mRNA Sample Preparation kit according to Illumina user guide (PN 15031047) with the following modifications: 2 min mRNA fragmentation and 12 cycles library PCR amplification. Libraries were then sequenced on an Illumina HiSeq 4000 system using single-end 1 × 50 bases. Image analysis and base calling were performed using RTA 2.7.3 and bcl2fastq 2.17.1.14. Reads were mapped onto mm10 assembly of mouse genome using Tophat v2.0.14 (Kim et al., 2013) and bowtie2 v2.1.0 aligner (Langmead and Salzberg, 2012). Quantification of gene expression was performed using HTSeq v0.6.1 (Anders et al., 2015) using gene annotations from Ensembl release 81. Normalization and differential gene expression analysis were performed using R and DESeq2 v1.6.3 Bioconductor library (Love et al., 2014). Principal Component Analysis were computed on regularized logarithm transformed data for each stage, calculated with the method proposed by Love et al. 2014, using all genes expressed in at least one represented sample. Unsupervised hierarchical clustering (Pearson correlation, average linkage) and heat maps were performed using Heatmapper (Babicki et al., 2016; http://www.heatmapper.ca;).

2.5. Real–time quantitative polymerase chain reaction

One microgram of total RNA was used to synthesize cDNA using Iscript reverse transcriptase (IscriptTM Reverse Transcription Supermix for RT-qPCR, Bio-Rad) as specified by the manufacturer. Quantitative PCR was performed on a CFX96 Real-time System (Bio-Rad) using iQ SYBR Green supermix (Bio-Rad). PCR was performed as follow: 95 °C for 30 s, followed by 40 cycles of 4 s at 95 °C and 4 s at 60 °C. Three standard genes (Actin *[Acta]*, Tata-box binding protein [*Tbp*] and RNA polymerase 2 subunit [*Pol II*]) were used and data were normalized with GeNorm softwarev3.5. Primer sequences are given in supplementary table 1.

2.6. Pathway analysis

Gene enrichment analysis was performed by using Gene Ontology and Consensus Pathway Data Base. For theses analyses of the CHMP2B^{intron5} mice, genes with an adjusted *p*-value lower than 0.05 and a fold change (FC) value < 0.67 for down-regulated or > 1.5 for up-regulated genes were selected. Pathway over-representation composed of at least 3 genes and with an adjusted *p*-value < 0.05 was considered as significantly altered.

2.7. Statistical analysis

Unless otherwise indicated, data are expressed as the mean ± SEM. GraphPad Prism version 6.0a software was used for statistical analysis. Tests used are indicated in the legends under the figures. Differences with *p*-values < 0.05 were considered significant. The statistical significance of the overlap between the lists of significantly differentially expressed genes in CHMP2B^{intron5} and SOD1 mice was computed using an hypergeometric test.

3. Results

3.1. Deregulated genes in the spinal cord of CHMP2B^{intron5} mice: transcriptomic analysis discriminate between CHMP2B^{intron5} Tg mice and nTg mice at the three stages of the disease

To gain insight into the nature and extent of gene expression changes occurring in ALS-FTD syndrome linked to CHMP2B^{intron5} mutation in mice, the spinal cord transcriptomes of Tg and age-matched nTg mice were studied by RNA-sequencing at three stages of disease progression: AS stage (1.5 month of age, no motor symptom) S stage (6 months of age, signs of hindlimb weakness) and the E stage of the disease (10–12 months of age, hindlimb paralysis or loss of the righting reflex).

Principal component analysis (PCA) performed with the ~34,000 expressed genes for each stage showed a clear discrimination between genotypes at AS and E stages. This segregation was less pronounced at S stage probably reflecting an heterogeneity of disease progression between Tg mice (Fig. 1). Indeed, S stage represents an intermediate situation where all mice are not necessarily at the same stage of disease development even if hindlimb weakness is seen. To improve the analysis, we then selected the deregulated genes with an adjusted *p*-value < 0.05. As shown in Table 1 the number of deregulated genes with an adjusted *p*-value < 0.05 increased with disease progression.

Table 1
Summary of the number of deregulated genes with the sequentially applied cut-off.

Cut-off stage	Number of significantly deregulated genes	
	$p < 0.05$	$p < 0.05$
		FC ≤0.67 or ≥ 1.5
Asymptomatic (1.5 month)	1063	281
Symptomatic (6 months)	2809	576
End-stage (10 months)	4404	348

Using this first cut-off, unsupervised hierarchical clustering showed that these differentially expressed genes segregated all the Tg mice from their nTg littermates as shown by the dendrograms in Fig. 2A. To highlight the most altered cellular processes, a fold change (FC) value < 0.67 for down-regulated or > 1.5 for up-regulated genes and an adjusted *p*-value < 0.05 were used as criteria for defining a set of deregulated candidate genes in Tg when compared to nTg mice. Comparison of gene expression resulted in 281, 576 and 348 differentially regulated genes at the AS, S and E stage respectively (Table 1). Interestingly, as disease progressed, the percentage of up-regulated genes in Tg mice was decreased while the percentage of down-regulated genes was increased when compared to nTg littermates (Fig. 2B). Complete lists of genes found either up- or down-regulated in Tg when compared to nTg mice are given in supplementary tables 2–4. Among the deregulated genes identified, 49 were common to the three time points with 19 up-regulated and 30 repressed (Fig. 2C).

To ascertain RNA-sequencing results, gene expression was then assessed by RT-qPCR on an independent cohort of mice. For each stage, 10 genes were selected on the basis of their FC. Expression levels of the selected transcripts obtained by RT-qPCR were comparable with the FC

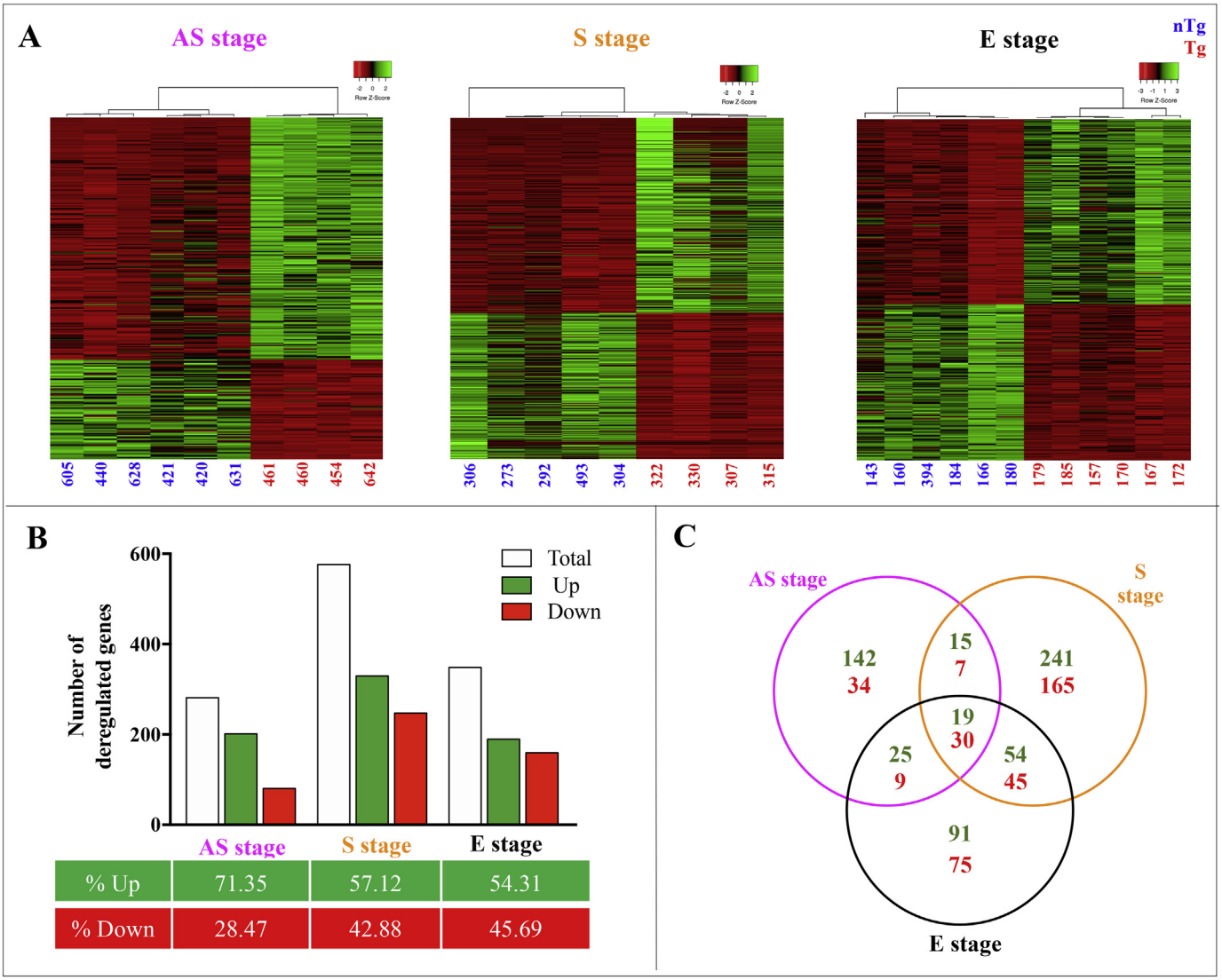

Fig. 2. Evolution of transcriptomic profile with disease progression. Genes differentially expressed with an adjusted *p-value* < 0.05 and a fold change < 0.67 or > 1.5 were analyzed. A: Heatmap and hierachical clustering analysis profiles of Tg and nTg mice at the three stages studied. Scaled expression values are coloured-code according to the legend on the top right. Dendrograms depict hierarchical clustering based on differentially expressed genes and show a complete separation between genotypes at the three stages of the disease.
B. Distribution of genes with altered expression at the three stages studied in Tg vs nTg mice. White bar: total number of genes with deregulated expression, green bar: up-regulated genes, red bar: downregulated genes. The table represents the percentage of up- and down-regulated genes for each stage.
C. Venn diagram summarizing genes overlapping between the three stages.
Green: up-regulated genes, Red: down-regulated genes. nTg: non transgenic mice; Tg: CHMP2B^{intron5}.
transgenic mice. (For interpretation of the references to colour in this figure legend, the reader is referred to the web version of this article.)

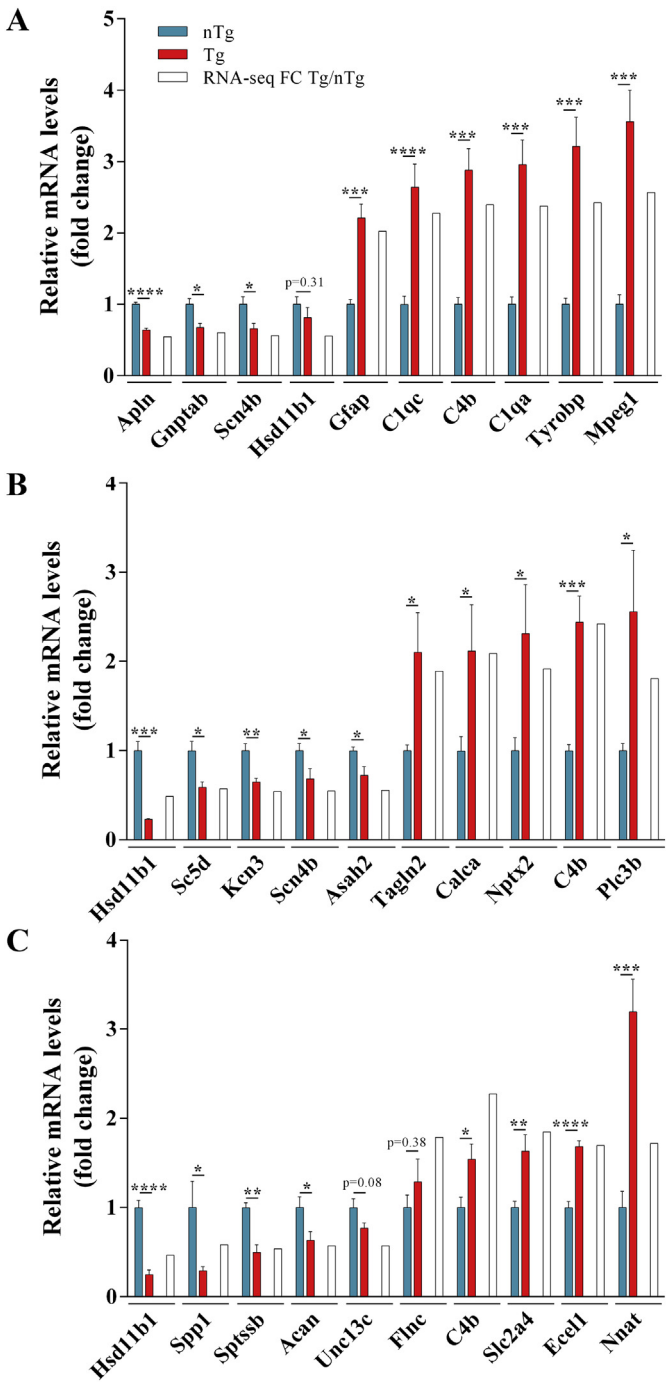

Fig. 3. Validation of RNA-seq results by RT-qPCR.
For each stage, asymptomatic (A), symptomatic (B) and end stage (C) expression of 10 genes either up- or down-regulated in the RNAseq analysis was measured by RT-qPCR in an independent cohort. For the RT-qPCR graphs represent means ± SEM. For the RNAseq graphs represent the fold change (FC). qPCR: n = 6–7 per genotype; RNAseq: n = 4–6 per genotype. $^{*}p < 0.05$, $^{**}p < 0.01$, $^{***}p < 0.001$, $^{****}p < 0.0001$, Student's t-test.

found by RNA-seq analysis except for 3 genes, *Hsd11b1* at AS stage and *Unc13* (p =0.079) and *Flnc* at ES stage whose regulation did not reach significance (Fig. 3).

3.2. Transcriptomic profiles evolve as disease progresses

In an attempt to identify the mechanisms altered throughout the course of the disease and the pathways with a significant number of differentially expressed genes, gene ontology analysis was performed with significantly dysregulated genes.

At the AS stage, while no evident histological changes are found in the spinal cord (supplementary fig. 1), two major pathways emerged as over-represented: the immune system (34% of the deregulated genes; over-representation: p_{adj} = 2.1e-14) and the metabolism of lipids (9.6% of the deregulated genes, over-representation: p_{adj} = 1.10e-03). Among the 95 deregulated genes linked to the immune process 32 of them were associated with the inflammatory response (Table 2). Remarkably, except for *Cxcl9* that was down-regulated, the 31 other genes involved in inflammatory response were induced. The most up-regulated proinflammatory and chemo attractant molecules were *Ccl3*, *Ccl4* and *Ccl6* (FC > 3.8), followed by complement subunits *C1qa*, *C1qb*, *C1qc*, *C4b* (FC > 2.2) and *C3* and *C4a* (FC > 1.5) and its receptor *C3ar1* (FC = 2.01), and other receptors (*Fcer1g*, *Fcgr1*, *Csf1r*, *Ptafr* and *Tlr2*).

In addition, we showed an increase of *Trem2* (FC = 3.1) a type I transmembrane protein primarily expressed in microglia in the central nervous system and of its protein adaptor *Tyrobp* (FC = 2.42), as well as of other lectin-related inflammatory proteins such as *Lgals3* (FC = 3.39), *Clec7a* (FC = 3.06) and the integrin *Itgax* (FC = 5).

The second pathway identified as over-represented dealt with the metabolism of lipids (Table 3), a pathway known to be altered in ALS (Dupuis et al., 2008). Indeed, among the 281 deregulated genes, 27 genes belong to the lipid metabolism process with 13 genes down-regulated and 14 genes up-regulated. These deregulated genes were involved in plasma lipoprotein assembly, remodeling, and clearance, cholesterol metabolism, synthesis of very long-chain fatty acyl-CoAs and steroids metabolism (Table 3).

Six lipases were deregulated: 60 kDa lysophospholipase (*Aspg*: FC = 2.19), lipoprotein lipase (*Lpl*: FC = 1.9), phospholipase D4 (*Pld4*: FC = 1.73), phospholipase B1 (*Plb1*: FC = 1.53) endothelial lipase (*Lipg*: FC = 0.64) and phospholipase A2 (*Pla2g3*: FC = 0.58).

The two apolipoproteins *Apoc1* and *Apoe* were up-regulated with a FC of respectively 2.34 and 1.75 while cubilin (*Cubn*) a protein that mediates high density lipoproteins transport was down-regulated (FC = 0.65).

In addition, three enzymes involved in the metabolism of sphingolipids were down regulated: the serine palmitoyltransferase small subunit B (*Sptssb*: FC = 0.62), a subunit of serine palmitoyltranferase that catalyzes the first step in the biosynthesis of sphingolipids, the sphingosine-1-phosphate phosphatase 2 (*Sgpp2*: FC = 0.65) responsible of sphingosine-1-phosphate synthesis and the 2-hydroxyacylsphingosine 1-beta-galactosyltransferase (*Utg8a*: FC = 0.65) which catalyzes the synthesis of galactosylceramide from ceramide. Finally, *Hexb*, the beta subunit of hexosaminidase that converts ganglioside GM2 to GM3 was over-expressed (FC = 1.52). Four genes involved in steroid metabolism were down-regulated: the corticosteroid 11-beta-dehydrogenase isozyme 1 (*Hsd11b1*: FC = 0.55) which converts cortisone into corticosterone, 3-alpha-hydroxysteroid dehydrogenase type 1 (*Akr1c4*: FC = 0.64) that mediates neurosteroids synthesis, hydroxymethylglutaryl-CoA synthase (*Hmgcs1*: FC = 0.66) and isopentenyl-diphosphate delta-isomerase 1(*Idil1*: FC = 0.66) that both participate to cholesterol synthesis. Two were up-regulated: testosterone 17-beta-dehydrogenase 3 (*Hsd17b3*: FC = 1.75) which converts androstenedione in testosterone and ATP-binding cassette, sub-family C (CFTR/MRP), member 3 (*Abcc3*: FC = 1.79) which is a multidrug-resistance transporter that mediates efflux of 17-beta-glucuronosyl estradiol and organic cations.

At the S stage (Table 4), when motor impairments are obvious, the mainly altered processes were related to neuronal system/activity. Indeed, 43 genes associated with this process were deregulated (7.4% of the deregulated genes; over-representation: p_{adj} = 6.3e-6). Most of them were related to electrical activity of the neuron including potassium and sodium channels, neurotransmitter receptors or transporters and axon guidance. Potassium channels represent the most complex class of voltage-gated ion channels from both functional and structural

Table 2
Deregulated genes of the immune system at the asymptomatic stage. Spinal cords from CHMP2B^{intron5} mice were compared to non-transgenic littermates. ↑: up-regulated gene; ↓: down-regulated gene.

Gene name	Description	Fold change	Adjusted *p*-value	Inflammation	Complement coagulation cascade	Macrophage markers
Aif1	Allograft inflammatory factor 1	1.64	5.2e-06	↑		
Arl11	ADP-ribosylation factor-like protein 11	2.84	1.9e-15			
Batf3	Basic leucine zipper transcriptional factor ATF-like 3	1.89	2.6e-04			
Bcl3	B-cell lymphoma 3 protein homolog	1.64	1.2e-02			
Blnk	B-cell linker protein	1.72	1.3e-05			
C1qa	Complement C1q subcomponent subunit A	2.38	4.7e-10		↑	
C1qb	Complement C1q subcomponent subunit B	2.21	1.7e-12		↑	
C1qc	Complement component 1, q subcomponent, C chain	2.28	9.8e-10		↑	
C3	Complement component 3	1.80	1.5e-09	↑	↑	
C3ar1	Complement component 3a receptor 1	2.01	5.7e-06	↑	↑	
C4a	Complement component 4A	1.56	1.49e-03	↑	↑	
C4b	Complement component 4B	2.39	2.7e-21		↑	
Ccl3	C-C motif chemokine 3	3.82	2.3e-16	↑		
Ccl4	C-C motif chemokine 4	3.82	2.3e-16	↑		
Ccl6	C-C motif chemokine 6	4.60	1.2e-22	↑		
Cd109	CD109 antigen	2.23	7.3e-10			
Cd14	CD14 antigen	1.97	3.0e-07	↑		↑
Cd180	CD180 antigen	2.02	1.1e-06	↑		
Cd22	CD22 antigen	1.61	1.8e-02			
Cd300lb	CD300 molecule like family member B	1.74	5.3e-03			
Cd44	CD44 antigen	1.57	2.7e-03	↑		
Cd48	CD48 antigen	1.72	4.6e-04			
Cd52	CD52 antigen	1.80	5.7e-04			↑
Cd68	CD68 antigen	2.77	2.3e-24			↑
Cd84	CD84 antigen	1.96	2.0e-06			
Clec7a	C-type lectin domain family 7, member a	3.06	1.62e-13			
Csf1r	Macrophage colony-stimulating factor 1 receptor	1.57	1.4e-10	↑		
Csf3r	Granulocyte colony-stimulating factor receptor	2.05	4.3e-12			
Ctsd	Cathepsin D	1.58	1.2e-11			
Ctss	Cathepsin S	1.92	2.2e-08			
Ctsz	Cathepsin Z	1.55	1.1e-08			
Cx3cr1	CX3C chemokine receptor 1	1.53	5.7e-06	↑		
Cxcl9	C-X-C motif chemokine 9	0.61	1.0e-02	↓		
Cyba	Cytochrome b-245 light chain	1.65	7.3e-03			
Dcstamp	Dendritic cell-specific transmembrane protein	1.60	3.3e-02			
Endou	Poly(U)-specific endoribonuclease	2.07	1.3e-12			
Enpp3	Ectonucleotide pyrophosphatase/phosphodiesterase family member 3	0.62	1.6e-03			
Fbxo40	F-box protein 40	0.60	4.2e-05			
Fcer1g	High affinity immunoglobulin epsilon receptor subunit gamma	1.93	1.6e-07	↑		
Fcgr1	High affinity immunoglobulin gamma Fc receptor I	1.51	3.6e-04	↑		
Fcgr3	Low affinity immunoglobulin gamma Fc region receptor III	1.87	2.7e-07	↑		
Fgr	Tyrosine-protein kinase Fgr	1.59	1.9e-02			
Fyb	FYN-binding protein	1.51	1.2e-03			
Gpr183	G protein coupled receptor 183	1.56	1.3e-03			
Gpr84	G protein-coupled receptor 84	1.66	1.2e-02			
H2-Oa	Histocompatibility 2, O region alpha locus	1.59	3.4e-02			
H2-Ob	Histocompatibility 2, O region beta locus	1.85	1.2e-06			
Havcr2	Hepatitis A virus cellular receptor 2 homolog	1.91	2.8e-07	↑		
Hcar2	Hydroxycarboxylic acid receptor 2	1.86	9.6e-04			
Hexb	Hexosaminidase B	1.52	2.4e-06			
Hvcn1	Hydrogen voltage-gated channel 1	1.86	5.2e-06			
Il1a	Interleukin-1 alpha	1.61	2.6e-02	↑		
Il1rn	Interleukin-1 receptor antagonist protein	1.71	6.3e-03	↑		
Irf5	Interferon regulatory factor 5	1.57	3.9e-05			
Irf8	Interferon regulatory factor 8	1.81	1.5e-06			
Itgax	Integrin alpha-X	5.02	2.2e-24		↑	
Itgb2	Integrin beta-2	1.63	3.3e-04	↑	↑	
Lag3	Lymphocyte-activation gene 3	2.16	8.4e-09			
Lat2	Linker for activation of T-cells family member 2	1.58	2.2e-05			
Lgals3	Galectin-3	3.39	3.8e-23			
Lrrc17	Leucine-rich repeat-containing protein 17	1.64	2.1e-02			
Ly86	Lymphocyte antigen 86	1.53	3.1e-02	↑		
Ly9	T-lymphocyte surface antigen Ly-9	1.68	1.2e-03			
Lyz2	Lysozyme 2	1.52	1.1e-02			↑
Mpeg1	Macrophage expressed gene 1	2.57	4.17e-13			↑
Myo1f	Unconventional myosin-If	1.82	1.4e-06			
Naip2	Baculoviral IAP repeat-containing protein 1b	1.67	2.0e-04	↑		
Naip5	Baculoviral IAP repeat-containing protein 1e	1.98	1.1e-09	↑		
Naip6	Baculoviral IAP repeat-containing protein 1f	1.70	2.8e-03	↑		
Nckap1l	Nck-associated protein 1-like	1.54	3.8e-06			

(*continued on next page*)

Table 2 (*continued*)

Gene name	Description	Fold change	Adjusted *p*-value	Inflammation	Complement coagulation cascade	Macrophage markers
Nme2	NME/NM23 nucleoside diphosphate kinase 2	1.50	1.6e-02			
Pdcd1	Programmed cell death protein 1	4.37	2.5e-21			
Pitx2	Pituitary homeobox 2	1.54	4.3e-02			
Pla2g3	Phospholipase A2, group III	0.58	9.4e-05			
Plau	Plasminogen activator, urokinase	1.76	1.3e-06		↑	
Pld4	Phospholipase D4	1.73	1.7e-08			
Ptafr	Platelet-activating factor receptor	1.75	5.1e-08	↑		
Ptprq	Phosphatidylinositol phosphatase PTPRQ	0.55	1.1e-03			
Ptx3	Pentraxin-related protein PTX3	2.47	4.2e-13			
Serpinf2	Serpin f2	2.57	5.7e-08	↑	↑	
Siglecf	Sialic acid binding Ig-like lectin F	1.62	2.2e-02			
Six4	Homeobox protein SIX4	0.63	4.5e-04			
Slamf8	SLAM family member 8	1.78	2.8e-03	↑		
Slc11a1	Natural resistance-associated macrophage protein 1	2.16	3.6e-19	↑		
Thy1	Thy-1 membrane glycoprotein	2.39	2.5e-27			
Ticam2	TIR domain-containing adapter molecule 2	1.54	3.2e-02	↑		
Timp1	Metalloproteinase inhibitor 1	2.32	1.2e-07	↑		
Tlr2	Toll-like receptor 2	2.02	2.0e-12	↑		
Tnfaip8l2	Tumor necrosis factor alpha-induced protein 8-like protein 2	1.70	4.2e-05			
Tnfrsf1a	Tumor necrosis factor receptor superfamily, member 1a	1.51	1.7e-06	↑		
Tnfsf8	Tumor necrosis factor ligand superfamily member 8	1.74	3.9e-03			
Trem2	Triggering receptor expressed on myeloid cells 2	3.08	2.6e-27			
Tyrobp	TYRO protein tyrosine kinase-binding protein	2.42	3.6e-13			
Unc93b1	Protein unc-93 homolog B1	1.53	3.2e-03			
Zbtb16	Zinc finger and BTB domain containing 16	0.59	9.7e-03			

standpoints. They play a crucial role in maintaining membrane potential and modulating electrical excitability in neurons. Thirteen potassium channel subunits or potassium channel-related genes were deregulated. *Kcnh4*, *Kcnj4*, *Kcnmb1, Kcns1, Kcnv1* and *Hcn3* and *Gnb3* mRNAs were up-regulated while *Kcna1, Kcna2 Kcnc3, Kcng4*, *Hcn2* and *Abcc9* mRNAs were repressed. Sodium channels expression was also altered. Voltage-gated sodium channels subunits alpha *Scn9a, Scn10a, Scn11a* and nicotinic receptor subunits *Chrna6* and *Chrnb3* mRNAs were up-regulated. In contrast voltage-gated sodium channel ß subunit *Scn4b* and nicotinic receptor alpha2 subunit *Chrna2* mRNAs were repressed. In addition sodium-coupled neurotransmitter transporters were also identified. *Slc17a7* encoding the vesicular glutamate transporter VGLUT1 and *Slc6a12* encoding the GABA transporter GAT2 were up-regulated. At the same time, *Slc6a4* encoding the serotonin transporter SERT and *Slc6a5* encoding the glycine transporter GLYT2 were repressed. In addition, *Slc1a2* (FC = 0.72, not included in Table 3), encoding the glutamate transporter EAAT2 was also repressed but does not reached our FC threshold. Finally, mRNAs encoding GABA receptor rho2 subunit *Gabrr2* was up regulated while GABA receptor ß2 subunit *Gabrb2* and glycine receptor α1 subunit *Glra1* were down regulated in Tg when compared to nTg mice.

At E stage deregulation of neuronal system (4.3% of the deregulated genes, over-representation: p_{adj} = 0.038) was still present (Table 5). However, the number of deregulated genes was decreased when compared to S stage falling from 43 to 15 genes. Potassium channels family remained the most represented family with 6 out of 15 genes identified. In addition to the neuronal system, a new pathway linked with extracellular matrix emerged (Table 6). In this pathway mRNAs encoding collagens (*Col6a, Col9a3, Col20a1* and *Col 27a1*) were up-regulated while mRNAs encoding integrins were either up- (*Itgad, Itgax*) or down-regulated (*Itga1, Itgb3*) and proteoglycans *Acan* and *Hapln* were down-regulated.

In independent control experiments, mRNA levels of neuronal markers were measured by RT-qPCR in order to determine whether the effects seen on the above mentioned neuronal genes were due to a neuronal loss. As shown on supplementary fig. 2 expression levels of the 7 different neuronal genes tested were unchanged in Tg compared to nTg mice. The absence of obvious neuronal loss was confirmed by NeuN immunostaining.

To complete our analyses, we studied the progression of genes expression from the over-represented families. We studied the profile of each gene and classified the genes according to their expression level as compared to nTg mice, throughout the course of the disease. For each family and each stage, the number of deregulated genes and the corresponding percentage of genes either up- or down-regulated or with an unchanged expression are summarized in Table 7 and the full list of genes is given in supplementary table 5. As shown in Fig. 4, for the families that were over-represented at the AS stage, an expression pattern showing an initial up-regulation of this group of genes before returning to an expression level comparable to nTg mice largely prevailed. Indeed, 71% and 33% of the genes for the immune system/inflammation and lipid metabolism respectively showed this pattern of expression. Interestingly, in both families the percentage of over-expressed genes at AS was strongly decreased at S stage (< 10%) but re-increased up to 16.8% and 18.5% in both family at the E stage. In contrast, if the percentage of down-regulated genes was stable (3%) at the S and E stage for the immune system, it represented around 22% of the genes of the lipid metabolism family initially found deregulated. For the genes belonging to the neuronal system that were over-represented at S stage, the expression pattern that prevailed (~40% of the genes) showed an up-regulation limited to this stage with a normal level of expression at AS and E stages. The deregulated genes represented ~15% and ~35% of the family at the AS and E stages with a majority of repressed genes. For the two over-represented families at the E stage a common expression pattern prevailed with a normal expression level at the AS and S stages followed by an up-regulation at the E stage. These genes represented ~27% and ~46% of the deregulated genes for the neuronal system and the ECM respectively. For the neuronal system, a second pattern corresponding to a normal level of expression at the A stage followed by a down regulation at the S and E stages was seen for ~27% of the genes. The percentage of up-regulated genes increased progressively from AS (~7%) to E stage (~47%) while the percentage of repressed genes was stable at AS and S stages (~13%) and was increased by 4-folds at E stage. For the ECM family, the percentage of up-regulated genes was stable at AS and S stages (~8%) and was increased by 8-folds at E stage while the percentage of repressed genes increased

Table 3
Deregulated genes involved in the lipid metabolism at the asymptomatic stage. Spinal cords from CHMP2B^{intron5} mice were compared to non-transgenic littermates. ↑: up-regulated gene; ↓: down-regulated gene.

Gene name	Description	Fold change	adjusted *p*-value	Plasma lipoprotein assembly, remodeling, and clearance	Cholesterol metabolism	Synthesis of very long-chain fatty acyl-CoAs	Steroids metabolism
A2m	Alpha-2-macroglobulin	1.55	5.16e-05	↑			
Abcc3	ATP-binding cassette. Sub-family C (CFTR/MRP). member 3	1.79	4.48e-08				↑
Akr1c4	3-alpha-hydroxysteroid dehydrogenase type 1	0.64	1.53e-02				↓
Apoc1	Apolipoprotein C-I	2.34	4.58e-10	↑	↑		
Apoe	Apolipoprotein E	1.75	1.99e-04	↑	↑		
Aspg	60 kDa lysophospholipase	2.19	1.67e-08				
Cubn	Cubilin	0.65	1.97e-03	↓			↓
Elovl2	Elongation of very long chain fatty acids protein 2	0.66	4.19e-07			↓	
Gpd1	Glycerol-3-phosphate dehydrogenase [NAD(+)]. cytoplasmic	0.65	1.58e-07				
Hexb	Beta-hexosaminidase subunit beta	1.52	2.41e-06				
Hmgcs1	Hydroxymethylglutaryl-CoA synthase. Cytoplasmic	0.66	7.36e-06		↓		↓
Hpgds	Hematopoietic prostaglandin D synthase	1.69	9.44e-08				
Hsd11b1	Corticosteroid 11-beta-dehydrogenase isozyme 1	0.55	2.87e-10				↓
Hsd17b3	Testosterone 17-beta-dehydrogenase 3	1.75	3.22e-03			↑	↑
Idi1	Isopentenyl-diphosphate Delta-isomerase 1	0.66	2.25e-04		↓		↓
Ip6k3	Inositol hexakisphosphate kinase 3	1.61	1.21e-04				
Lipg	Endothelial lipase	0.64	4.50e-02	↓	↓		
Lpl	Lipoprotein lipase	1.90	1.99e-04	↑	↑		
Pla2g3	Phospholipase A2. group III	0.58	9.40e-05				
Plb1	Phospholipase B1. membrane-associated	1.53	3.79e-02				
Pld4	Phospholipase D4	1.73	1.67e-08				
Sgpp2	Sphingosine-1-phosphate phosphatase 2	0.65	8.10e-08				
Sptssb	Serine palmitoyltransferase small subunit B	0.62	5.60e-08				
Tecrl	Trans-2.3-enoyl-CoA reductase-like	0.63	2.13e-02			↓	
Tnfaip8l2	Tumor necrosis factor. Alpha-induced protein 8-like 2	1.70	4.24e-05				
Tnfrsf1a	Tumor necrosis factor receptor superfamily member 1A	1.51	1.75e-06				
Ugt8a	2-hydroxyacylsphingosine 1-beta-galactosyltransferase	0.65	3.11e-03				

Table 4
Deregulated genes involved in the neuronal system at the symptomatic stage. Spinal cords from CHMP2B^{intron5} mice were compared to non-transgenic littermates. ↑: up-regulated gene; ↓: down-regulated gene.

Gene name	Description	Fold change	Adjusted *p*-value	K^+ channels	Voltage-gated K^+ channels	Cholinergic receptors	Neurotransmitter transporters & transmission accross chemical synapse	Phase 0 rapid depolarization	Axon guidance
Abcc9	ATP-binding cassette, sub-family C (CFTR/MRP), member 9	0.65	1.20e-03	↓					
Cacnb3	Calcium channel, voltage-dependent, beta 3 subunit	1.62	2.70e-04				↑	↑	↑
Chrna2	Cholinergic receptor, nicotinic, alpha polypeptide 2 (neuronal)	0.32	4.30e-21			↓	↓		
Chrna6	Cholinergic receptor, nicotinic, alpha polypeptide 6	2.03	3.11e-05			↑	↑		
Chrnb3	Cholinergic receptor, nicotinic, beta polypeptide 3	1.68	1.41e-03			↑	↑		
Col6a1	Collagen, type VI, alpha 1	1.54	2.20e-04						↑
Cxcl12	Chemokine (C-X-C motif) ligand 12	0.65	1.62e-03						↓
Dcc	Deleted in colorectal carcinoma	0.57	7.94e-04						↓
Dok4	Docking protein 4	2.13	7.65e-06						↑
Dok6	Docking protein 6	0.67	2.92e-02						↓
Epha6	Eph receptor A6	0.66	1.78e-02						↓
Gabrb2	Gamma-aminobutyric acid (GABA) A receptor, subunit beta 2	0.61	7.74e-03				↓		
Gabrr2	Gamma-aminobutyric acid (GABA) C receptor, subunit rho 2	1.77	2.35e-03				↑		
Gfra3	Glial cell line derived neurotrophic factor family receptor alpha 3	2.84	2.80e-10						↑
Glra1	Glycine receptor, alpha 1 subunit	0.56	8.24e-04				↓		
Gnb3	Guanine nucleotide binding protein (G protein), beta 3	1.67	2.69e-03	↑			↑		
Hcn2	Hyperpolarization-activated, cyclic nucleotide-gated K+ 2	0.64	1.72e-04	↓					
Hcn3	Hyperpolarization-activated, cyclic nucleotide-gated K+ 3	1.58	2.89e-03	↑					
Htr3b	5-hydroxytryptamine (serotonin) receptor 3B	1.72	3.77e-03				↑		
Isl2	Insulin related protein 2 (islet 2)	2.17	1.29e-05						↑
Itga1	Integrin alpha 1	0.64	6.44e-03						↓
Itga2	Integrin alpha 2	0.66	3.94e-02						↓
Itgb3	Integrin beta 3	0.67	3.10e-04						↓
Kcna1	Potassium voltage-gated channel, shaker-related subfamily, member 1	0.61	1.47e-09	↓	↓				
Kcna2	Potassium voltage-gated channel, shaker-related subfamily, member 2	0.64	5.62e-11	↓	↓				
Kcnc3	Potassium voltage gated channel, Shaw-related subfamily, member 3	0.54	4.08e-14	↓	↓				
Kcng4	Potassium voltage-gated channel, subfamily G, member 4	0.65	1.96e-05	↓	↓				
Kcnh4	Potassium voltage-gated channel, subfamily H (eag-related), member 4	1.64	2.04e-03	↑	↑				
Kcnj4	Potassium inwardly-rectifying channel, subfamily J, member 4	1.52	3.62e-02	↑			↑		
Kcnmb1	Potassium large conductance calcium-activated channel, subfamily M, beta member 1	1.58	6.65e-03	↑					
Kcns1	K+ voltage-gated channel, subfamily S, 1	1.63	3.90e-04	↑	↑				
Kcnv1	Potassium channel, subfamily V, member 1	1.53	1.92e-02	↑	↑				
Plcb3	Phospholipase C, beta 3	1.81	8.03e-05				↑		
Robo1	Roundabout homolog 1	0.64	4.94e-06						↓
Scn10a	Scn10a: sodium channel, voltage-gated, type X, alpha	2.15	3.89e-15					↑	↑

(*continued on next page*)

Table 4 (*continued*)

Gene name	Description	Fold change	Adjusted *p*-value	K^+ channels	Voltage-gated K^+ channels	Cholinergic receptors	Neurotransmitter transporters & transmission accross chemical synapse	Phase 0 rapid depolarization	Axon guidance
Scn11a	Scn11a: sodium channel, voltage-gated, type XI, alpha	3.51	7.51e-26					↑	↑
Scn4b	Scn4b: sodium channel, type IV, beta	0.55	2.59e-17					↓	↓
Scn9a	Scn9a: sodium channel, voltage-gated, type IX, alpha	2.03	2.58e-05					↑	↑
Slc17a7	Solute carrier family 17 (sodium-dependent inorganic phosphate cotransporter), member 7	3.42	3.80e-23				↑		
Slc6a12	Solute carrier family 6 (neurotransmitter transporter, betaine/GABA), member 12	1.52	1.60e-02				↑		
Slc6a4	Solute carrier family 6 (neurotransmitter transporter, serotonin), member 4	0.64	2.03e-02				↓		
Slc6a5	Solute carrier family 6 (neurotransmitter transporter, glycine), member 5	0.61	5.54e-08				↓		
Unc5b	Unc-5 homolog B	0.66	3.38e-04						↓

Table 5
Deregulated genes of the neuronal system at the end stage. Spinal cords from $CHMP2B^{intron5}$ mice were compared to non-transgenic littermates. ↑: up-regulated gene; ↓: down-regulated gene.

Gene name	Description	Fold change	Adjusted *p*-value	K^+ channels	Voltage-gated K^+ channels	Cholinergic receptors	Transmission accross chemical synapse
Chrna2	Cholinergic receptor nicotinic alpha 2 subunit	0.27	1.70e-33			↓	↓
Chrnb4	Cholinergic receptor nicotinic beta 4 subunit	1.57	9.04e-05			↑	↑
Gabrr2	Gamma-aminobutyric acid type A receptor rho2 subunit	2.63	1.59e-09				↑
Glrb	Glycine receptor beta	0.65	3.26e-05				↓
Hcn2	Hyperpolarization activated cyclic nucleotide gated potassium and sodium channel 2	0.68	1.24e-04	↓			
Hcn3	Hyperpolarization activated cyclic nucleotide gated potassium channel 3	1.54	1.13e-03	↑			
Kcna1	Potassium voltage-gated channel subfamily A member 1	0.61	4.17e-12	↓	↓		
Kcna2	Potassium voltage-gated channel subfamily A member 2	0.65	7.61e-13	↓	↓		
Kcnc3	Potassium voltage-gated channel subfamily C member 3	0.60	1.85e-12	↓	↓		
Kcnh4	Potassium voltage-gated channel subfamily H member 4	1.53	2.69e-03	↑	↑		
Kcnh7	Potassium voltage-gated channel subfamily H member 7	0.66	1.92e-03	↓	↓		
Kcnk7	Potassium two pore domain channel subfamily K member 7	1.65	5.95e-03	↑			
Kcns3	Potassium voltage-gated channel modifier subfamily S member 3	0.66	1.36e-09	↓	↓		
Prkcg	Protein kinase C gamma	1.53	2.54e-08				↑
Slc18a3	Solute carrier family 18 member A3, vesicular transporter of acetylcholine	1.53	3.14e-03				↑

Table 6
Deregulated genes involved in the extracellular matrix at the end stage. Spinal cords from CHMP2B^{intron5} mice were compared to non-transgenic littermates. ↑: up-regulated gene; ↓: down-regulated gene.

Gene name	Description	Fold change	Adjusted *p*-value	Collagen biosynthesis and modifying enzymes	Integrin cell surface interactions	Proteoglycan
Acan	Aggrecan	0.57	3.67e-16			↓
Adamts14	A disintegrin-like and metallopeptidase with thrombospondin type 1 motif, 14	1.57	3e-04	↑		
Bmp1	Bone morphogenetic protein 1	1.58	2e-05	↑		
Col20a1	Collagen, type XX, alpha 1	1.51	1e-03	↑		
Col27a1	Collagen, type XXVII, alpha 1	1.64	3e-05	↑		
Col6a1	Collagen, type VI, alpha 1	1.54	2e-04	↑		
Col9a3	Collagen, type IX, alpha 3	1.52	3e-03	↑	↑	
Hapln1	Hyaluronan and proteoglycan link protein 1	0.46	9.82e-13			↓
Itga1	Integrin alpha 1	0.60	4e-04		↓	
Itgad	Integrin, alpha D	1.98	9e-05		↑	
Itgax	Integrin alpha X	1.94	2e-04		↑	
Itgb3	Integrin beta 3	0.63	1e-06		↓	
Spp1	Secreted phosphoprotein 1	0.58	7e-07		↓	

progressively from AS (~15%) to E stage (~38%).

Finally, in these over-represented families, 8 genes were constantly up-regulated while 12 were constantly down-regulated (supplementary table 5).

In order to further determine the genes that were constantly deregulated during disease progression, irrespective of the over-represented families, we compared the deregulated genes at the three stages. Forty-nine genes common to AS, S and E stages were found (Table 8). Twelve genes were related to the neuronal system (*Chrna2, Hspb1, Kcnc3, Kcnh4, Nnat, Pdlim4, Scn4b, Slc6a5, Sspo, Steap2, Strip1, Uts2*), 5 were linked to lipid metabolism (*Apoc1, Gpd1, Hsd11b1, Sptssb, Ugt8a*), 4 were linked to the immune system (*C4a, C4b, Lgals3, Thy1*) and 2 were related to ECM (*Acan, Hapln1*). In addition, a new category related to transcription became apparent with the induction of the transcriptional regulators *Atf3, Batf3*, *Prrx2* and *Wisp2* and the down-regulation of histone methyl transferase *Smyd1*. Interestingly all the identified genes were either up- or down-regulated over the three stages. Among the repressed genes, 11 were of unknown function.

Table 7
Table showing the percentage of genes up-regulated (FC > 1.5), non deregulated (FC [0.67–1.5] or down-regulated (FC < 0.67) for the over-represented families at the three stages of the disease. Grey boxes indicate the stage of over-representation. For each stage, the number of deregulated genes and the total number of genes in the family are indicated into bracket.

Over-represented family	FC	AS	S	E
Immune system Inflammation	>1.5	92.6 % (88/95)	9.5 % (9/95)	16.8 % (16/95)
	[0.67-1.5]	0 % (0/95)	87.4 % (83/95)	80 % (76/95)
	<0.67	7.4 % (7/95)	3.1 % (3/95)	3.2 % (3/95)
Lipid metabolism	>1.5	51.8 % (14/27)	7.4 % (2/27)	18.5 % (5/27)
	[0.67-1.5]	0 % (0/27)	70.3 % (19/27)	59.2 % (16/27)
	<0.67	48.2 % (13/27)	22.3 % (6/27)	22.3 % (6/27)
Neuronal system	>1.5	4.6 % (2/43)	51.2 % (22/43)	9.3 % (4/43)
	[0.67-1.5]	86 % (37/43)	0 % (0/43)	65.1 % (28/43)
	<0.67	9.4 % (2/43)	48.8 % (21/43)	25.6 % (11/43)
Neuronal system	>1.5	6.7 % (1/15)	20 % (3/15)	46.6 % (7/15)
	[0.67-1.5]	80 % (12/15)	66.7 % (10/15)	0 % (0/15)
	<0.67	13.3 % (2/15)	13.3 % (2/15)	53.4 % (8/15)
ECM	>1.5	7.7 % (1/13)	7.7 % (1/13)	61.5 % (8/13)
	[0.67-1.5]	76.9 % (10/13)	69.2 % (9/13)	0 % (0/13)
	<0.67	15.3 % (2/13)	23.1 % (3/13)	38.5 % (5/13)

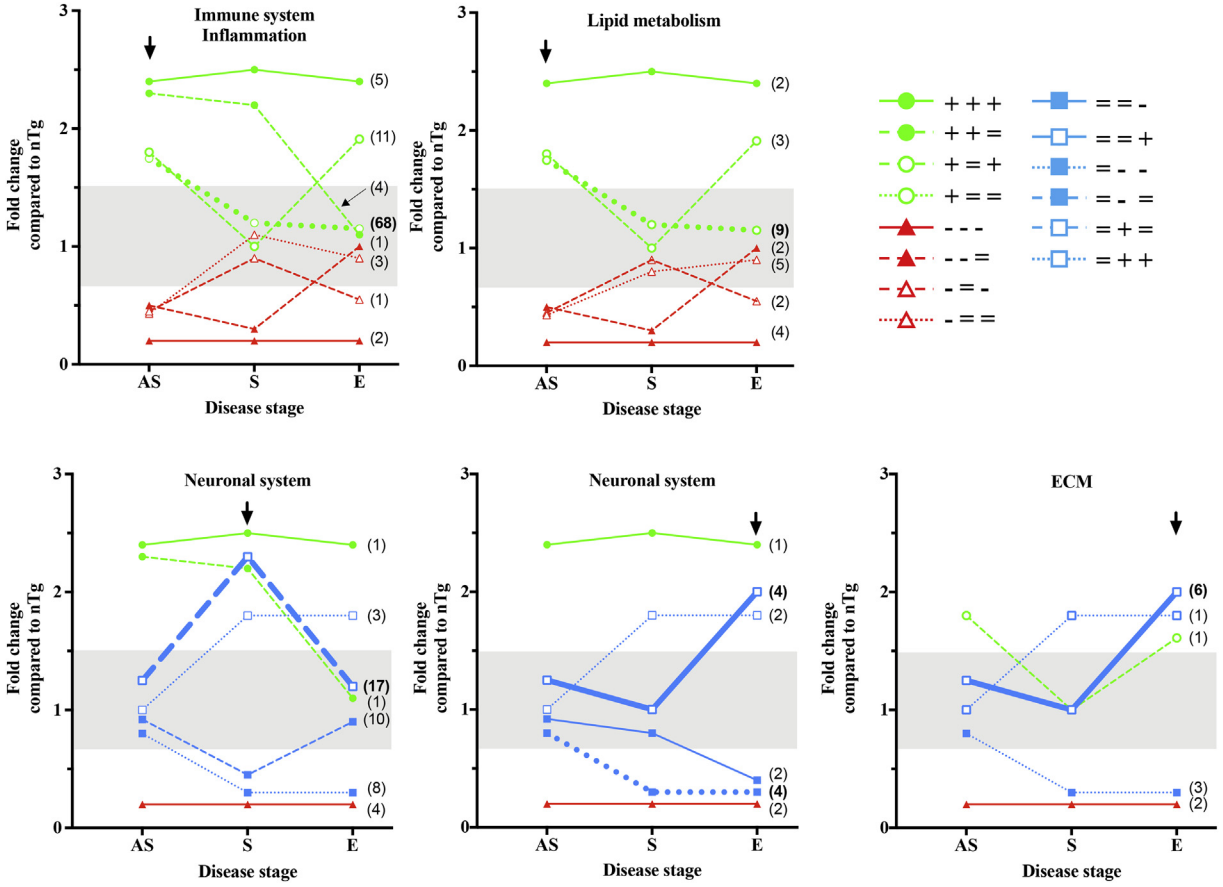

Fig. 4. Representative patterns of gene expression changes through disease progression for the genes of the over-represented families.
For each family, the most represented pattern is shown in bold line. The number of genes for each pattern is indicated into brackets. Arrows indicate the stage of over-representation. Grey rectangle indicates the zone where fold change is considered non significant. AS: asymptomatic stage, S: symptomatic stage, E: end stage. +: up-regulated, =: comparable to nTg, −: downregulated.

3.3. CHMP2B^{intron5} and SOD1^{G86R} mice share common deregulated genes at symptomatic stage of the disease

In an attempt to investigate overlapping alterations in gene expression profiles and highlight pathological mechanisms common to two ALS-related mutants, we compared our results obtained on spinal cord from CHMP2B^{intron5} mice at S stage with those of transcriptomic analyses performed on spinal cord from SOD1^{G86R} mice at 90 days of age corresponding to the S stage, when mice develop signs of hindlimb weakness in this line. Using the same criteria than those used for CHMP2B^{intron5} model analysis, we found 449 deregulated genes in SOD1^{G86R} mice when compared to controls. Among them, 28 were common to both models, with 22 genes up-regulated, 3 genes down-regulated and 3 genes with opposite deregulations. The overlap between the lists of differentially expressed genes in CHMP2B^{intron5} and SOD1^{G86R} mice was statistically significant (p-value = 2.770336e-08, hypergeometric test). We then categorized these genes and identified 7 deregulated processes (see Table 9 for details). The most represented was the immune system including inflammatory response, followed by molecules involved in transcription, lipid metabolism, neuronal system, repression of translation and cell-cell interactions. Two genes were of unknown function.

4. Discussion

This work is the first study that thoroughly characterizes the transcriptomic changes that occur throughout the course of disease progression in the spinal cord of an ALS-FTD mouse model. This model that develops characteristic features of ALS at the motor and histological levels is based on the neuronal over-expression of the CHMP2B^{intron5}

Table 8
Genes deregulated at the three stages studied in spinal cord of CHMP2B^{intron5} mice when compared to non-transgenic littermates.

	Up	Down
Neuronal system	*Gpr179, Hspb1, Nnat, Pdlim4, Sspo, Uts2,*	*Chrna2, Kcn3, Kcnh4, Scn4b, Slc6a5, Steap2, Strip2*
Immune system	*C4a, C4b, Lgals3, Thy1*	
Lipid metabolism	*Apoc1*	*Gpd1, Hsd11b1, Sptssb, Ugt8a*
ECM		*Acan, Hapln1*
Transcription	*Atf3, Batf3, Prrx2, Wisp2*	*Smyd1*
Other	*Agt, Calcb, Cartpt*	*Apln, Aqp6, Atp2b1, Fbxo40, Mybpc3, Olfr287*
Unknown		*Gm45217000008O03Rik, 4930432E11Rik, 5031414D18Rik, A730020M07Rik, Gm10684, Gm15512, Gm21984, Gm26633, Gm26673, Gm33366, Gm4524*

Table 9
Common deregulated genes in spinal cord of CHMP2B^{intron5} and SOD1^{G86R} mice at symptomatic stage.

Process	Genes		
	Up	Down	Adverse regulation
Immune system Inflammatory response	*Calca, Calcb, Cd44, Clic, Endou, Gcnt2, Hcar2, Lgals3, Ly86, Slc7a7, Ucn, Tagln2*		*Spp1, Fcrls*
Transcription	*Atf3, Bcl3, Crym, Runx1, Wisp2*		*Slfn5*
Lipids and lipoproteins clearance	*Anxa2*	*Ugt8a*	
Neuronal system	*Gpr35, Hspb1*		
Translation repressor	*Eif4ebp1*		
Cell-cell interaction	*Ppl*		
Unknown function		*RIKEN cDNA 4930432E11 gene, RIKEN cDNA A730020M07 gene*	

mutant (Vernay et al., 2016). Using RNAseq followed by bioinformatic analysis we established that as early as 1.5 month of age, the transcriptomic profiles of CHMP2B^{intron5} Tg mice showed their own gene expression signature that differs from nTg mice. This demonstrates that transcriptomic changes, confirmed by RT-qPCR on an independent cohort, already exist several weeks before the first visible clinical motor symptoms. In this transgenic line, CHMP2B^{intron5} expression is driven by the Thy1.2 promoter, a promoter known to be neuron specific with a strong expression in motor and cortical neurons (Gordon et al., 1987). In Thy1.2-CRE transgenic mice, expression starts from E11 to E14 in the cortex depending on the transgenic line (Campsall et al., 2002). In Tg mice we found a cortical expression of the CHMP2B^{intron5} mutant concomitant with the expression of endogenous CHMP2B at the mRNA levels as early as E15 (data not shown). This early expression of the transgene concomitant with endogenous CHMP2B suggests a potential effect of the mutant protein early in the course of development as it could happen in patients carrying the mutant gene.

This transcriptomic profile of over-represented families among the deregulated genes evolves through the course of the disease with a progressive switch of deregulated pathways from immune system/inflammatory response and lipid metabolism to neuronal system and ECM when motor symptoms become visible.

4.1. Neuronal expression of CHMP2B^{intron5} triggers an initial inflammation with disruption of lipid metabolism before onset of motor symptoms

Inflammatory processes are strongly related to ALS and FTD but also to other neurodegenerative disorders such as Alzheimer's or Parkinson diseases. Their role in the development and progression of neurodegenerative diseases is however not clearly understood. Here, we report that neuronal expression of CHMP2B^{intron5} mutant triggers a strong activation of immune system associated with an activation of the inflammatory response in spinal cord before any motor symptoms. Indeed, transcripts encoding chemoattractant proteins CCL3, CCL4 and CCL6 that stimulate the recruitment of inflammatory cells (Schulthess et al., 2012) are induced together with an increase of microglial/macrophage or astrocyte markers (*Aif1/Iba1; Cx3cr1; Cd68; Cd14; Cd52; Gfap*). In addition expression of IL-1α and TNFα receptors, which are related to the proinflammatory pathway (Tortarolo et al., 2015), and complement cascade components are also up-regulated. These data are in agreement with the data obtained in another transgenic mouse line over-expressing CHMP2B^{intron5} under the prp promoter and in human *CHMP2B* mutation carriers. Indeed, Isaac's group demonstrated the presence of an early microgliosis in brain of CHMP2B^{intron5} mice with an up-regulation of mRNAs encoding inflammation markers including *Irf8* and *Csf1r* two genes overexpressed in our study (Clayton et al., 2017). Interestingly, in human *CHMP2B* mutation carriers, it was recently shown that serum levels of CCL4 are increased throughout life (Roos et al., 2018). In sporadic ALS patients CCL3, CCL4, IL-1α are increased in CSF while TNFα receptor levels are increased in plasma. In addition CCL6 is over-expressed in astrocytes from SOD1^{G37R} mouse model (Sun et al., 2015) and activation of complement cascade is also observed in SOD1^{G93A} mouse model (Ferraiuolo et al., 2007) and in serum of ALS patients (Apostolski et al., 1991). However, depletion of C1q or C3, two essential proteins of complement cascade, does not increase the lifespan of SOD1^{G37R} nor delay the degeneration of motor neurons (Lobsiger et al., 2013) suggesting that complement activation is a consequence rather than a cause of disease progression. We also highlight the activation of an inflammatory pathway based on TREM2. TREM2 was previously associated with both ALS pathogenesis (Cady et al., 2014) and microglial activation (Cantoni et al., 2015) and very recently with FTD caused by *CHMP2B* mutants (Roos et al., 2018). TREM2 is a cell surface receptor expressed by microglia, interacting with protein tyrosine kinase binding protein (TYROBP). This apoptotic cell-detector which recognizes a variety of ligands, is able to bind Apolipoprotein E (ApoE) (Bailey et al., 2015) and to promote proinflammatory mechanisms by the induction of inflammatory players (Krasemann et al., 2017). Interestingly, using microarray analysis, Cox and collaborators found that *ApoE* is over-expressed in motoneurons of human *CHMP2B* mutation carriers (Cox et al., 2010). Our results show the induction of *Trem2* and its interactor *Tyrobp* associated with an induction of *Apoe* and inflammatory markers including *Clec7a*, *Lgals3*, *Gpnmb* and *Itgax*. Interestingly, *Clec7a* is also over-expressed in astrocytes of SOD1^{G93A} ALS mouse model (Baker et al., 2015) while *Itgax* and *ApoE* are increased in microglia (Chiu et al., 2013). However, the exact consequence of TREM2 pathway activation is currently still a matter of debate. Indeed, recent data suggest a rather beneficial neuroprotective role of TREM2 by interacting with TLR2 and CD14, two genes that are both shown to be induced in the present study. Thus, whether TREM2 pathway activation is beneficial or deleterious in the pathological context linked to CHMP2B^{intron5} neuronal expression remains to be elucidated.

Lipids directly contribute to cell signaling, membrane stability/fluidity and neuronal energy balance during stress. It was recently shown that hyperlipidemia is a causal risk factor in ALS patients (Bandres-Ciga et al., 2019). Some recent lipidomic studies point toward a change in lipid metabolism in ALS-FTD patients characterized by an increase of circulating triglycerides level and cholesterol/HDL ratio, and a decrease of LDL and APOC1 (Ahmed et al., 2018; Kim et al., 2018a, 2018b). However little is known about human *CHMP2B* mutation carriers. Here, we show for the first time that early in the course of the disease, before any motor symptoms, that expression of genes implicated in the lipid metabolism are significantly altered in CHMP2B^{intron5} Tg mice. Indeed, expression of several genes encoding proteins involved in plasma lipoprotein formation and clearance, cholesterol metabolism, synthesis of very long chain fatty acids and steroid metabolism is altered. *Apo*e expression is increased as previously found in a transcriptomic analysis of motor neurons from human *CHMP2B* mutation carriers (Cox et al., 2010). However, in an experimental cellular model (IPSC-derived cortical neurons expressing *CHMP2B* mutant) an opposite result was obtained suggesting a potential importance of culture manipulations and conditions or the limits of such models

(Zhang et al., 2017). Lipidation of APOE can be performed by ABCA1 a membrane receptor mainly found in the plasma membrane of astrocytes that mediates the efflux of cholesterol and phospholipids to lipid-poor apolipoproteins (Wahrle et al., 2004). In the present transcriptomic analysis *Abca1* expression is also found to be induced (FC = 1.41) although not reaching the chosen threshold of significance. Nevertheless, this increase of *Abca1* could favor the transport of lipids by APOE to neurons and glia. Associated with these up-regulations of lipids import factors, LPL which hydrolyzes and transports free fatty-acids to neurons and schwann cells (Eckel and Robbins, 1984; Huey et al., 1998) is also induced suggesting an increase of lipids availability for these cells. Of note, gene expression profiling and proteomic analyses reported increased levels of LPL in mutant $SOD1^{G93A}$ mouse spinal cords. However, in our study other deregulations point toward an inhibition of lipids uptake. Indeed, APOC1, known as an APOE and LPL inhibitor (Berbee et al., 2005) is increased. APOC1 regulates activities of several proteins involved in high density lipoprotein metabolism and its over-expression provokes a hypertriglyceridemia in human and murine plasma composition through the inhibition of LPL activity. This increase of *ApoC1* is also found in the spinal cord of ALS patients, impacting the uptake of lipids by neurons and glial cells (D'Erchia et al., 2017).

The decreased expression of enzymes involved in the synthesis of cholesterol and very long chain fatty acids (*Hmgcs1, Idi1, Tecrl, Elovl2*) could lead to a global reduction of lipids bioavailability. *Hmgcs1* was found down regulated in a transcriptomic study performed on spinal cords from ALS patients (D'Erchia et al., 2017). We further observed a decrease of *Cubn* which is involved in the endocytosis of holoparticles of HDL (Hammad et al., 1999).

Finally, sphingolipids are involved in key pathways for ALS, such as autophagy and protein clearance, cell survival, energy metabolism, and neuroinflammation. Our analysis also identified two genes whose deregulation would deregulate the glycosphingolipid pathway: *Ugt8a* and *Hexb*. Interestingly, similar regulations were found in $SOD1^{G86R}$ mice, and *Ugt8a* expression level correlated with disease severity (Henriques et al., 2017a, 2017b). All these alterations in lipid metabolism may affect the cell metabolism and the organization of cellular membranes and, in turn, modify axon guidance and synaptic transmission participating to disease progression and neuronal dysfunction.

In the $CHMP2B^{intron5}$ mice, at the early stage of the disease, deregulation of the immune system and lipid metabolism are concomitant. Numerous data have already shown that these two processes can be linked by oxidative stress. Indeed, activated microglial cells increase ROS production (Haslund-Vinding et al., 2017; Peterson and Flood, 2012) leading to oxidation of lipids in the plasma membranes of the surrounding cells (de la Haba et al., 2013; Yang et al., 2006). This oxidation of membrane lipids promotes membrane curve disturbance and favors aggregates formation. Moreover, changes in composition of membrane lipids are also known to alter synaptic plasticity and trigger apoptosis (Ledesma et al., 2012). Cutler showed that oxidative stress leads to an increase of ceramide and cholesterol in ALS patients and that inhibition of ceramide and cholesterol synthesis protects against cell death induced by oxidative stress (Cutler et al., 2002). On the other hand, specific class of lipids such as prostaglandins or platelet activating factor (PAF) can also trigger inflammation. In our study, we observed an increased expression of *Plb1* that encodes an enzyme involved in the metabolism of glycerophosphocholine, a precursor of PAF (Edwards and Constantinescu, 2009; Marrache et al., 2002). In addition, *Ptafr*, encoding the PAF receptor expressed on cell surface of microglia (Aihara et al., 2000) is also over-expressed in our transgenic mice suggesting an activation of the PAF pathway.

Altogether, the results obtained at the asymptomatic stage suggest that activation of the immune system represents the initial step of disease onset. One possible cause could be the abnormal accumulation of protein aggregates due to neuronal expression of $CHMP2B^{intron5}$ that are already detectable at this stage and may trigger the inflammatory response, which then could further participate to neurotoxicity and disease progression. However, activation of immune system and inflammation is not specific to $CHMP2B^{intron5}$ mutant and seems to be a general mechanism in ALS, irrespective of the initial cause of the disease, similar activation being also found in sporadic ALS and FTD patients (McCauley and Baloh, 2018; Prado et al., 2018; Roos et al., 2018). The hypothesis of aggregate-causing inflammation has already been proposed for other neurodegenerative diseases and will be explored in the near future in this model. At this stage, the metabolism of lipid is also impacted by $CHMP2B^{intron5}$ neuronal expression. The emerging question is: which process impacts the other? Does the inflammatory response lead to the perturbation of lipid metabolism observed in ALS patients (Schmitt et al., 2014) or the reverse? Another hypothesis could be that proinflammation and lipid metabolism impairment are associated to generate a neurotoxic environment leading to neuronal dysfunction and neuronal death. As recalled above, oxidative stress could be the possible link between inflammation and lipid metabolism.

4.2. At the symptomatic and end stages, neuronal functions are deregulated

One of the characteristic features of ALS is the presence of muscle fasciculations. The origin of fasciculations depends on the functional state of lower motor neurons and is associated with an increase of their excitability (de Carvalho and Swash, 2017; de Carvalho et al., 2017).

A precise balance between neuronal excitation and inhibition is crucial for proper functioning of the nervous system. Disturbance of neuronal excitation-inhibition homeostasis results in severe pathological phenotypes, such as excitotoxic neurodegeneration, epilepsy, muscular spasticity, and mental retardation (Zoghbi et al., 2000). Electrical activity of the neuron and excitability are tightly link to the nature of ion channels expressed by the neuron. This homeostasis relies on the expression of ion channels, neurotransmitter receptors and transporters. So far the only study linking CHMP2B mutant to an alteration of neuronal functionality showed that mutant CHMP2B elicits a decrease in synaptic activity and suggest that the pathogenic proteins may perturb synaptic plasticity and microstructure, long before overt cell death (Belly et al., 2010). In this study, at symptomatic stage when motor symptoms are present in the $CHMP2B^{intron5}$ mice, we highlighted a major deregulation of genes implicated in the electrical activity of the neurons (i.e. potassium and sodium channels, neurotransmitter receptors and transporters) potentially leading to a hyperexcitability of the neurons. In support of this hypothesis *Kcna1* and *Kcna2,* that encode Kv1.1 and Kv1.2 alpha subunits voltage-gated potassium channels involved in repolarization and hyperpolarization of neurons by efflux of potassium ions, are down-regulated. *Kcna1* knock-out leads to a hyperexcitability of neurons with a lower excitation threshold without any change in resting potential (Brew et al., 2003) and mice develop seizures (Rho et al., 1999). In ALS patients *Kcna1* and *Kcna2* expression is decreased and correlates with hyperexcitability (Kanai et al., 2006; Kleine et al., 2008; Vucic and Kiernan, 2006), supporting the involvement of these two channels in the disease. In addition, *Scn10a* encodes Nav1.8 alpha subunit of a voltage-gated sodium channel that supports repetitive firing in response to sustained depolarization is increased, and gain-of-function mutations of Nav1.8 produce neurons hyperexcitability suggesting that over-expression of *Scn10a* could lead to hyperexcitability (Han et al., 2016). Interestingly, *Scn11a* that encodes the Nav1.9 voltage-gated sodium channel contributing to persistent hyperalgesia following exposure to inflammatory mediators (Huang et al., 2014) is increased in our study and in the transcriptomic study performed on motor neurons from human CHMP2B mutation carriers (Cox et al., 2010). As disease progresses, down-regulation of voltage-gated potassium channels persists while deregulation of sodium channels disappears.

We also observed a deregulation of the Slc family of proteins involved in neurotransmitters re-uptake. This deregulation of the Slc family is also observed in motor neurons from human CHMP2B carriers

(Cox et al., 2010) supporting the results obtained here with our model. In particular, *Slc6a4* involved in the re-uptake of serotonin is decreased, and in the spinal cord serotonin (5-HT) increases motoneuron excitability. Interestingly, the serotonin receptor 3b *Htr3b* is increased. In contrast, *Slc6a5* encoding the glycine transporter 2 (GLYT2) is decreased. It has been shown that in spinal cord of $SOD1^{G93A}$ ALS mice decreased GLYT2 expression is due to the degeneration of inhibitory interneurons possibly responsible for the hyperexcitability of motor neurons (Hossaini et al., 2011). Further, *Slc6a12* that codes GABA transporter involved in presynaptic GABA re-uptake is increased thereby possibly stopping GABA effect more rapidly. Moreover, *Slc17a7* that encodes the vesicular glutamate transporter 1 is increased in Cox study and in our study (Cox et al., 2010). Altogether one can hypothesizes that the convergence of these deregulations may drive a strong increase in neuronal excitability possibly initiating/participating to subsequent degeneration.

Finally, we also observed altered expression of genes related to extracellular matrix. Deregulation of collagen and integrin expressing genes was also reported in the transcriptomic study performed in motor neurons from human CHMP2B carriers (Cox et al., 2010). However, the consequences of these deregulations are not known and need to be further explored.

Interestingly, part of the genes of the over-represented families at one stage are also deregulated at the other stages. In particular, for the immune system-inflammation and the lipid metabolism families, a deregulation of respectively 20% and 40% of the genes initially deregulated at the AS stage is seen suggesting an involvement of these genes in the processes activated at E stage. Understanding why these genes are deregulated at the AS and E stages could give us some clues on the role of these genes in the pathogenesis.

The comparison of the deregulated genes at the three studied stages of the disease allowed us to identify constantly deregulated genes. Among these genes 49% belong to families or pathways already found deregulated at, at least, one studied stage. Among the remaining genes, one can notice that four transcription factors are commonly up-regulated: *Atf3* whose expression is increased in response to stress, *Batf3* whose expression is involved in dendritic cell differentiation, *Wisp2* that is up-regulated in ganglioside-deficient mice and though to have a neuroprotective function (Ohkawa et al., 2011) and *Prrx2* a member of the paired family of homeobox proteins. The role of the others deregulated genes in the pathogenesis remains to be elucidated.

Surprisingly, none of the pathways considered as responsible for the pathogenicity of CHMP2B mutants (i.e. *endo*-lysosomal pathway, autophagy) were found statistically over-represented when analyzed with the chosen threshold. This unexpected result may reflect the fact that our analysis was performed on the whole lumbar spinal cord while $CHMP2B^{intron5}$ expression was restricted to neurons. Nonetheless, considered individually, several genes related to these pathways (i.e. Rab, Atg, or cathepsins family members), were found deregulated strengthening the validity of our approach.

4.3. Comparison of transcriptomic profiles of $CHMP2B^{intron5}$ and $SOD1^{G86R}$ at symptomatic stage: identification of common new genes possibly involved in pathogenesis, irrespective of the genetic cause of the disease

If half of the identified genes common to the two ALS-causing mutants have already been associated with ALS or other neurodegenerative disorders (*AnxA* (Mishra et al., 2007), *Ugt8a* (Sevastou et al., 2016; Henriques et al., 2017a, 2017b)), *Atf3* (Malaspina et al., 2010; Vlug et al., 2005), *Bcl3* (Ferry et al., 2014), *Crym* (Daoud et al., 2011; Fukada et al., 2007), *Runx1* (Patel et al., 2011), *Wisp2* (Sevastou et al., 2016), *Calca* (de la Haba et al., 2013), *Calcb, Cd44* (Matsumoto et al., 2012), *Clic1* (Novarino et al., 2004), *Hcar2* (Wakade et al., 2014), *Spp1* (Morisaki et al., 2016; Yamamoto et al., 2017), *Lgals3* (Yan et al., 2016), *Hspb1* (Fukada et al., 2007; Gorter et al., 2018; Ylikallio et al., 2015)) the remaining genes have not been described as modified or involved in neurodegenerative diseases. However, they are related to physiological functions (immune system, neuronal system, lipid metabolism etc.…) known to be altered in neurodegenerative processes and in ALS in particular. Whether the change in expression of these genes is causative of the pathological process engaged by the two mutants or if it is a consequence has to be determined. Further work, including confirmation of changes at the protein level is now required in order to confirm whether they contribute to disease progression.

5. Conclusion

Our study is the first dynamic analysis of transcriptome in a $CHMP2B^{intron5}$ mouse model, a model developing characteristic hallmarks of ALS/FTD. Our RNA-Seq analysis of lumbar spinal cord provides a snapshot of transcriptomic events characterizing the disease at three different time points giving us an access to the very early changes engaged before motor symptoms become apparent but also to the variations of gene expression profile when motor symptoms become detectable and then when mice are paralyzed. Our results highlight an early deregulation of immune system and lipid metabolism at asymptomatic stage although transgene expression is limited to neurons.

How mutant drives these deregulations remains an open question. Understanding the mechanisms underlying these alterations and determining whether they are protective or deleterious are of prime importance to delineate new therapeutic strategies for these diseases with not cure.

We also show that appearance of motor symptoms correlate with the detectable deregulation of genes related to neuronal system and more specifically with genes involved in ions and neurotransmitters transport. These deregulations may underlie neuronal hyperexcitability that is thought to induce neuronal degeneration in ALS.

Finally the comparison of the gene expression signature of $CHMP2B^{intron5}$ mice with those of $SOD1^{G86R}$ mice at the symptomatic stage provides further insights into common underlying dysfunction of biological pathways, disrupted or disturbed in ALS.

It will now be interesting to test whether the genomic changes reported here have functional consequences at the level of the cognate proteins and then will then be reflected in changes in their activity. This will be particularly interesting for lipid metabolism pathway since their modification should be reflected by circulating metabolites (either in blood or CSF) and could then certainly serve as accessible biomarker for ALS, a presently unmet medical need.

In closing, our study provides a database for neuroscientists to explore potential candidate genes involved in the $CHMP2B^{intron5}$-based pathogenesis of ALS, and it may provide molecular clues to further understand the functional consequences that diseased neurons expressing CHMP2B mutant may have on their neighbor cells.

Declaration of competing interest

The authors declare that they have no conflict of interest.

Funding

This work was supported by funds from «Association pour la Recherche sur la Sclérose Latérale Amyotrophique et autres Maladies du Motoneurone» (FR), «Association pour la recherche et le développement de moyens de lutte contre les maladies neurodégénératives» (RW), «André Combat la SLA» (JPL), and Région Alsace (RW).

Acknowledgments

We thank Annie Picchinenna and Marie José Ruivo for excellent technical assistance. We also thank the “Plateforme Imagerie, Neuropôle de Strasbourg », for the technical assistance with confocal imaging.

Appendix A. Supplementary data

Supplementary data to this article can be found online at https://doi.org/10.1016/j.nbd.2019.104710.

References

Ahmed, R.M., Highton-Williamson, E., Caga, J., Thornton, N., Ramsey, E., Zoing, M., Kim, W.S., Halliday, G.M., Piguet, O., Hodges, J.R., Farooqi, I.S., Kiernan, M.C., 2018. Lipid metabolism and survival across the frontotemporal dementia-amyotrophic lateral sclerosis spectrum: relationships to eating behavior and cognition. J. Alzheimers Dis. 61, 773–783. https://doi.org/10.3233/JAD-170660.

Aihara, M., Ishii, S., Kume, K., Shimizu, T., 2000. Interaction between neurone and microglia mediated by platelet-activating factor. Genes Cells 5, 397–406. https://doi.org/10.1046/j.1365-2443.2000.00333.x.

Anders, S., Pyl, P.T., Huber, W., 2015. HTSeq – a Python framework to work with high-throughput sequencing data. Bioinformatics 31, 166–169. https://doi.org/10.1093/bioinformatics/btu638.

Apostolski, S., Nikolic, J., Bugarski-Prokopljevic, C., Miletic, V., Pavlovic, S., Filipovic, S., 1991. Serum and CSF immunological findings in ALS. Acta Neurol. Scand. 83, 96–98. https://doi.org/10.1046/j.1365-2443.2000.00333.x.

Babicki, S., Arndt, D., Marcu, A., Liang, Y., Grant, J.R., Maciejewski, A., Wishart, D.S., 2016. Heatmapper: web-enabled heat mapping for all. Nucleic Acids Res. 44 (W1), W147–W153. https://doi.org/10.1093/nar/gkw419. 2016 Jul 8.

Bailey, C.C., DeVaux, L.B., Farzan, M., 2015. The triggering receptor expressed on myeloid cells 2 binds apolipoprotein E. J. Biol. Chem. 290, 26033–26042. https://doi.org/10.1074/jbc.M115.677286.

Baker, D.J., Blackburn, D.J., Keatinge, M., Sokhi, D., Viskaitis, P., Heath, P.R., Ferraiuolo, L., Kirby, J., Shaw, P.J., 2015. Lysosomal and phagocytic activity is increased in astrocytes during disease progression in the SOD1 (G93A) mouse model of amyotrophic lateral sclerosis. Front. Cell. Neurosci. 9, 410. https://doi.org/10.3389/fncel.2015.00410.

Bandres-Ciga, S., Noyce, A.J., Hemani, G., Nicolas, A., Calvo, A., Mora, G., ITALSGEN Consortium, International ALS Genomics Consortium, Tienari, P.J., Stone, D.J., Nalls, M.A., Singleton, A.B., Chiò, A., Traynor, B.J., 2019. Shared polygenic risk and causal inferences in amyotrophic lateral sclerosis. Ann. Neurol. n85 (4), 470–481. https://doi.org/10.1002/ana.25431.

Belly, A., Bodon, G., Blot, B., Bouron, A., Sadoul, R., Goldberg, Y., 2010. CHMP2B mutants linked to frontotemporal dementia impair maturation of dendritic spines. J. Cell Sci. 123, 2943–2954. https://doi.org/10.1242/jcs.068817.

Berbee, J.F., van der Hoogt, C.C., Sundararaman, D., Havekes, L.M., Rensen, P.C., 2005. Severe hypertriglyceridemia in human APOC1 transgenic mice is caused by apoC-I-induced inhibition of LPL. J. Lipid Res. 46, 297–306. https://doi.org/10.1194/jlr.M400301-JLR200.

Brew, H.M., Hallows, J.L., Tempel, B.L., 2003. Hyperexcitability and reduced low threshold potassium currents in auditory neurons of mice lacking the channel subunit Kv1.1. J. Physiol. 548, 1–20. https://doi.org/10.1113/jphysiol.2002.035568.

Cady, J., Koval, E.D., Benitez, B.A., Zaidman, C., Jockel-Balsarotti, J., Allred, P., Baloh, R.H., Ravits, J., Simpson, E., Appel, S.H., Pestronk, A., Goate, A.M., Miller, T.M., Cruchaga, C., Harms, M.B., 2014. TREM2 variant p.R47H as a risk factor for sporadic amyotrophic lateral sclerosis. JAMA Neurol. 71, 449–453. https://doi.org/10.1001/jamaneurol.2013.6237.

Campsall, K.D., Mazerolle, C.J., De Repentingy, Y., Kothary, R., Wallace, V.A., 2002. Characterization of transgene expression and Cre recombinase activity in a panel of Thy-1 promoter-Cre transgenic mice. Dev. Dyn. 224 (2), 135–143.

Cantoni, C., Bollman, B., Licastro, D., Xie, M., Mikesell, R., Schmidt, R., Yuede, C.M., Galimberti, D., Olivecrona, G., Klein, R.S., Cross, A.H., Otero, K., Piccio, L., 2015. TREM2 regulates microglial cell activation in response to demyelination in vivo. Acta Neuropathol. 129, 429–447. https://doi.org/10.1007/s00401-015-1388-1.

Chassefeyre, R., Martinez-Hernandez, J., Bertaso, F., Bouquier, N., Blot, B., Laporte, M., Fraboulet, S., Coute, Y., Devoy, A., Isaacs, A.M., Pernet-Gallay, K., Sadoul, R., Fagni, L., Goldberg, Y., 2015. Regulation of postsynaptic function by the dementia-related ESCRT-III subunit CHMP2B. J. Neurosci. 35, 3155–3173. https://doi.org/10.1523/JNEUROSCI.0586-14.2015.

Chiu, I.M., Morimoto, E.T., Goodarzi, H., Liao, J.T., O'Keeffe, S., Phatnani, H.P., Muratet, M., Carroll, M.C., Levy, S., Tavazoie, S., Myers, R.M., Maniatis, T., 2013. A neurodegeneration-specific gene-expression signature of acutely isolated microglia from an amyotrophic lateral sclerosis mouse model. Cell Rep. 4, 385–401. https://doi.org/10.1016/j.celrep.2013.06.018.

Clayton, E.L., Mancuso, R., Nielsen, T.T., Mizielinska, S., Holmes, H., Powell, N., Norona, F., Larsen, J.O., Milioto, C., Wilson, K.M., Lythgoe, M.F., Ourselin, S., Nielsen, J.E., Johannsen, P., Holm, I., Collinge, J., FreJa, O.P.L., Gomez-Nicola, D., Isaacs, A.M., 2017. Early microgliosis precedes neuronal loss and behavioural impairment in mice with a frontotemporal dementia-causing CHMP2B mutation. Hum. Mol. Genet. 26, 873–887. https://doi.org/10.1093/hmg/ddx003.

Cox, L.E., Ferraiuolo, L., Goodall, E.F., Heath, P.R., Higginbottom, A., Mortiboys, H., Hollinger, H.C., Hartley, J.A., Brockington, A., Burness, C.E., Morrison, K.E., Wharton, S.B., Grierson, A.J., Ince, P.G., Kirby, J., Shaw, P.J., 2010. Mutations in CHMP2B in lower motor neuron predominant amyotrophic lateral sclerosis (ALS). PLoS One 5, e9872. https://doi.org/10.1371/journal.pone.0009872.

Cutler, R.G., Pedersen, W.A., Camandola, S., Rothstein, J.D., Mattson, M.P., 2002. Evidence that accumulation of ceramides and cholesterol esters mediates oxidative stress-induced death of motor neurons in amyotrophic lateral sclerosis. Ann. Neurol. 52, 448–457. https://doi.org/10.1002/ana.10312.

Daoud, H., Valdmanis, P.N., Gros-Louis, F., Belzil, V., Spiegelman, D., Henrion, E., Diallo, O., Desjarlais, A., Gauthier, J., Camu, W., Dion, P.A., Rouleau, G.A., 2011. Resequencing of 29 candidate genes in patients with familial and sporadic amyotrophic lateral sclerosis. Arch. Neurol. 68, 587–593. https://doi.org/10.1001/archneurol.2010.351.

de Carvalho, M., Swash, M., 2017. Physiology of the fasciculation potentials in amyotrophic lateral sclerosis: which motor units fasciculate? J. Physiol. Sci. 67, 569–576. https://doi.org/10.1007/s12576-016-0484-x.

de Carvalho, M., Kiernan, M.C., Swash, M., 2017. Fasciculation in amyotrophic lateral sclerosis: origin and pathophysiological relevance. J. Neurol. Neurosurg. Psychiatry 88, 773–779. https://doi.org/10.1136/jnnp-2017-315574.

de la Haba, C., Palacio, J.R., Martinez, P., Morros, A., 2013. Effect of oxidative stress on plasma membrane fluidity of THP-1 induced macrophages. Biochim. Biophys. Acta 1828, 357–364. https://doi.org/10.1016/j.bbamem.2012.08.013.

D'Erchia, A.M., Gallo, A., Manzari, C., Raho, S., Horner, D.S., Chiara, M., Valletti, A., Aiello, I., Mastropasqua, F., Ciaccia, L., Locatelli, F., Pisani, F., Nicchia, G.P., Svelto, M., Pesole, G., Picardi, E., 2017. Massive transcriptome sequencing of human spinal cord tissues provides new insights into motor neuron degeneration in ALS. Sci. Rep. 7, 10046. https://doi.org/10.1038/s41598-017-10488-7.

Dupuis, L., Corcia, P., Fergani, A., Gonzalez De Aguilar, J.L., Bonnefont-Rousselot, D., Bittar, R., Seilhean, D., Hauw, J.J., Lacomblez, L., Loeffler, J.P., Meininger, V., 2008. Dyslipidemia is a protective factor in amyotrophic lateral sclerosis. Neurology 70, 1004–1009. https://doi.org/10.1212/01.wnl.0000285080.70324.27.

Eckel, R.H., Robbins, R.J., 1984. Lipoprotein lipase is produced, regulated, and functional in rat brain. Proc. Natl. Acad. Sci. U. S. A. 81, 7604–7607.

Edwards, L.J., Constantinescu, C.S., 2009. Platelet activating factor/platelet activating factor receptor pathway as a potential therapeutic target in autoimmune diseases. Inflamm. Allergy Drug Targets 8, 182–190. https://doi.org/10.2174/187152809788681010.

Ferraiuolo, L., Heath, P.R., Holden, H., Kasher, P., Kirby, J., Shaw, P.J., 2007. Microarray analysis of the cellular pathways involved in the adaptation to and progression of motor neuron injury in the SOD1 G93A mouse model of familial ALS. J. Neurosci. 27, 9201–9219. https://doi.org/10.1523/JNEUROSCI.1470-07.2007.

Ferry, A., Joanne, P., Hadj-Said, W., Vignaud, A., Lilienbaum, A., Hourde, C., Medja, F., Noirez, P., Charbonnier, F., Chatonnet, A., Chevessier, F., Nicole, S., Agbulut, O., Butler-Browne, G., 2014. Advances in the understanding of skeletal muscle weakness in murine models of diseases affecting nerve-evoked muscle activity, motor neurons, synapses and myofibers. Neuromuscul. Disord. 24, 960–972. https://doi.org/10.1016/j.nmd.2014.06.001.

Fukada, Y., Yasui, K., Kitayama, M., Doi, K., Nakano, T., Watanabe, Y., Nakashima, K., 2007. Gene expression analysis of the murine model of amyotrophic lateral sclerosis: studies of the Leu126delTT mutation in SOD1. Brain Res. 1160, 1–10. https://doi.org/10.1016/j.brainres.2007.05.044.

Gascon, E., Gao, F.B., 2014. The emerging roles of microRNAs in the pathogenesis of frontotemporal dementia-amyotrophic lateral sclerosis (FTD-ALS) spectrum disorders. J. Neurogenet. 28, 30–40. https://doi.org/10.3109/01677063.2013.876021.

Gascon, E., Lynch, K., Ruan, H., Almeida, S., Verheyden, J.M., Seeley, W.W., Dickson, D.W., Petrucelli, L., Sun, D., Jiao, J., Zhou, H., Jakovcevski, M., Akbarian, S., Yao, W.D., Gao, F.B., 2014. Alterations in microRNA-124 and AMPA receptors contribute to social behavioral deficits in frontotemporal dementia. Nat. Med. 20, 1444–1451. https://doi.org/10.1038/nm.3717.

Ghanim, M., Guillot-Noel, L., Pasquier, F., Jornea, L., Deramecourt, V., Dubois, B., Le Ber, I., Brice, A., French Research Network on F.T.D. and Ftd/Mnd, 2010. CHMP2B mutations are rare in French families with frontotemporal lobar degeneration. J. Neurol. 257, 2032–2036. https://doi.org/10.1007/s00415-010-5655-8.

Ghazi-Noori, S., Froud, K.E., Mizielinska, S., Powell, C., Smidak, M., Fernandez de Marco, M., O'Malley, C., Farmer, M., Parkinson, N., Fisher, E.M., Asante, E.A., Brandner, S., Collinge, J., Isaacs, A.M., 2012. Progressive neuronal inclusion formation and axonal degeneration in CHMP2B mutant transgenic mice. Brain 135, 819–832. https://doi.org/10.1093/brain/aws006.

Gordon, J.W., Chesa, P.G., Nishimura, H., Rettig, W.J., Maccari, J.E., Endo, T., Seravalli, E., Seki, T., Silver, J., 1987. Regulation of Thy-1 gene expression in transgenic mice. Cell 50, 445–452.

Gorter, R.P., Stephenson, J., Nutma, E., Anink, J., de Jonge, J.C., Baron, W., Jahreibeta, M.C., Belien, J.A.M., van Noort, J.M., Mijnsbergen, C., Aronica, E., Amor, S., 2018. Rapidly progressive amyotrophic lateral sclerosis is associated with microglial reactivity and small heat shock protein expression in reactive astrocytes. Neuropathol. Appl. Neurobiol. https://doi.org/10.1111/nan.12525.

Hallmann, A.L., Arauzo-Bravo, M.J., Mavrommatis, L., Ehrlich, M., Ropke, A., Brockhaus, J., Missler, M., Sterneckert, J., Scholer, H.R., Kuhlmann, T., Zaehres, H., Hargus, G., 2017. Astrocyte pathology in a human neural stem cell model of frontotemporal dementia caused by mutant TAU protein. Sci. Rep. 7, 42991. https://doi.org/10.1038/srep42991.

Hammad, S.M., Stefansson, S., Twal, W.O., Drake, C.J., Fleming, P., Remaley, A., Brewer Jr., H.B., Argraves, W.S., 1999. Cubilin, the endocytic receptor for intrinsic factor-vitamin B(12) complex, mediates high-density lipoprotein holoparticle endocytosis. Proc. Natl. Acad. Sci. U. S. A. 96, 10158–10163.

Han, C., Huang, J., Waxman, S.G., 2016. Sodium channel Nav1.8: emerging links to human disease. Neurology 86, 473–483. https://doi.org/10.1212/WNL.0000000000002333.

Hand, C.K., Rouleau, G.A., 2002. Familial amyotrophic lateral sclerosis. Muscle Nerve 25, 135–159.

Haslund-Vinding, J., McBean, G., Jaquet, V., Vilhardt, F., 2017. NADPH oxidases in oxidant production by microglia: activating receptors, pharmacology and association with disease. Br. J. Pharmacol. 174, 1733–1749. https://doi.org/10.1111/bph.13425.

Henriques, A., Croixmarie, V., Bouscary, A., Mosbach, A., Keime, C., Boursier-Neyret, C., Walter, B., Spedding, M., Loeffler, J.P., 2017a. Sphingolipid metabolism is dysregulated at transcriptomic and metabolic levels in the spinal cord of an animal model of amyotrophic lateral sclerosis. Front. Mol. Neurosci. 10, 433. https://doi.org/10.3389/fnmol.2017.00433.

Henriques, A., Huebecker, M., Blasco, H., Keime, C., Andres, C.R., Corcia, P., Priestman, D.A., Platt, F.M., Spedding, M., Loeffler, J.P., 2017b. Inhibition of beta-glucocerebrosidase activity preserves motor unit integrity in a mouse model of amyotrophic lateral sclerosis. Sci. Rep. 7, 5235. https://doi.org/10.1038/s41598-017-05313-0.

Hossaini, M., Cardona, C.S., van Dis, V., Haasdijk, E.D., Hoogenraad, C.C., Holstege, J.C., Jaarsma, D., 2011. Spinal inhibitory interneuron pathology follows motor neuron degeneration independent of glial mutant superoxide dismutase 1 expression in SOD1-ALS mice. J. Neuropathol. Exp. Neurol. 70, 662–677. https://doi.org/10.1097/NEN.0b013e31822581ac.

Huang, J., Han, C., Estacion, M., Vasylyev, D., Hoeijmakers, J.G., Gerrits, M.M., Tyrrell, L., Lauria, G., Faber, C.G., Dib-Hajj, S.D., Merkies, I.S., Waxman, S.G., Group, P.S., 2014. Gain-of-function mutations in sodium channel Na(v)1.9 in painful neuropathy. Brain 137, 1627–1642. https://doi.org/10.1093/brain/awu079.

Huey, P.U., Marcell, T., Owens, G.C., Etienne, J., Eckel, R.H., 1998. Lipoprotein lipase is expressed in cultured Schwann cells and functions in lipid synthesis and utilization. J. Lipid Res. 39, 2135–2142.

Kanai, K., Kuwabara, S., Misawa, S., Tamura, N., Ogawara, K., Nakata, M., Sawai, S., Hattori, T., Bostock, H., 2006. Altered axonal excitability properties in amyotrophic lateral sclerosis: impaired potassium channel function related to disease stage. Brain 129, 953–962. https://doi.org/10.1093/brain/awl024.

Kim, D., Pertea, G., Trapnell, C., Pimentel, H., Kelley, R., Salzberg, S.L., 2013. TopHat2: accurate alignment of transcriptomes in the presence of insertions, deletions and gene fusions. Genome Biol. 14, R36. https://doi.org/10.1186/gb-2013-14-4-r36.

Kim, W.S., He, Y., Phan, K., Ahmed, R.M., Rye, K.A., Piguet, O., Hodges, J.R., Halliday, G.M., 2018a. Altered high density lipoprotein composition in behavioral variant frontotemporal dementia. Front. Neurosci. 12, 847. https://doi.org/10.3389/fnins.2018.00847.

Kim, W.S., Jary, E., Pickford, R., He, Y., Ahmed, R.M., Piguet, O., Hodges, J.R., Halliday, G.M., 2018b. Lipidomics analysis of behavioral variant frontotemporal dementia: a scope for biomarker development. Front. Neurol. 9, 104. https://doi.org/10.3389/fneur.2018.00104.

Kleine, B.U., Stegeman, D.F., Schelhaas, H.J., Zwarts, M.J., 2008. Firing pattern of fasciculations in ALS: evidence for axonal and neuronal origin. Neurology 70, 353–359. https://doi.org/10.1212/01.wnl.0000300559.14806.2a.

Krasemann, S., Madore, C., Cialic, R., Baufeld, C., Calcagno, N., El Fatimy, R., Beckers, L., O'Loughlin, E., Xu, Y., Fanek, Z., Greco, D.J., Smith, S.T., Tweet, G., Humulock, Z., Zrzavy, T., Conde-Sanroman, P., Gacias, M., Weng, Z., Chen, H., Tjon, E., Mazaheri, F., Hartmann, K., Madi, A., Ulrich, J.D., Glatzel, M., Worthmann, A., Heeren, J., Budnik, B., Lemere, C., Ikezu, T., Heppner, F.L., Litvak, V., Holtzman, D.M., Lassmann, H., Weiner, H.L., Ochando, J., Haass, C., Butovsky, O., 2017. The TREM2-APOE pathway drives the transcriptional phenotype of dysfunctional microglia in neurodegenerative diseases. Immunity 47https://doi.org/10.1016/j.immuni.2017.08.008. 566–581 e9.

Krasniak, C.S., Ahmad, S.T., 2016. The role of CHMP2B^{Intron5} in autophagy and frontotemporal dementia. Brain Res. 1649 (Pt B), 151–157. https://doi.org/10.1016/j.brainres.2016.02.051.

Krokidis, M.G., Vlamos, P., 2018. Transcriptomics in amyotrophic lateral sclerosis. Front. Biosci. (Elite Ed.) 10, 103–121.

Langmead, B., Salzberg, S.L., 2012. Fast gapped-read alignment with bowtie 2. Nat. Methods 9, 357–359. https://doi.org/10.1038/nmeth.1923.

Ledesma, M.D., Martin, M.G., Dotti, C.G., 2012. Lipid changes in the aged brain: effect on synaptic function and neuronal survival. Prog. Lipid Res. 51, 23–35. https://doi.org/10.1016/j.plipres.2011.11.004.

Lillo, P., Hodges, J.R., 2009. Frontotemporal dementia and motor neurone disease: overlapping clinic-pathological disorders. J. Clin. Neurosci. 16, 1131–1135. https://doi.org/10.1016/j.jocn.2009.03.005.

Ling, S.C., Polymenidou, M., Cleveland, D.W., 2013. Converging mechanisms in ALS and FTD: disrupted RNA and protein homeostasis. Neuron 79, 416–438. https://doi.org/10.1016/j.neuron.2013.07.033.

Lobsiger, C.S., Boillee, S., Pozniak, C., Khan, A.M., McAlonis-Downes, M., Lewcock, J.W., Cleveland, D.W., 2013. C1q induction and global complement pathway activation do not contribute to ALS toxicity in mutant SOD1 mice. Proc. Natl. Acad. Sci. U. S. A. 110, E4385–E4392. https://doi.org/10.1073/pnas.1318309110.

Love, M.I., Huber, W., Anders, S., 2014. Moderated estimation of fold change and dispersion for RNA-seq data with DESeq2. Genome Biol. 15, 550. https://doi.org/10.1186/s13059-014-0550-8.

Malaspina, A., Ngoh, S.F., Ward, R.E., Hall, J.C., Tai, F.W., Yip, P.K., Jones, C., Jokic, N., Averill, S.A., Michael-Titus, A.T., Priestley, J.V., 2010. Activation transcription factor-3 activation and the development of spinal cord degeneration in a rat model of amyotrophic lateral sclerosis. Neuroscience 169, 812–827. https://doi.org/10.1016/j.neuroscience.2010.04.053.

Marrache, A.M., Gobeil Jr., F., Bernier, S.G., Stankova, J., Rola-Pleszczynski, M., Choufani, S., Bkaily, G., Bourdeau, A., Sirois, M.G., Vazquez-Tello, A., Fan, L., Joyal, J.S., Filep, J.G., Varma, D.R., Ribeiro-Da-Silva, A., Chemtob, S., 2002. Proinflammatory gene induction by platelet-activating factor mediated via its cognate nuclear receptor. J. Immunol. 169, 6474–6481. https://doi.org/10.4049/jimmunol.169.11.6474.

Matsumoto, T., Imagama, S., Hirano, K., Ohgomori, T., Natori, T., Kobayashi, K., Muramoto, A., Ishiguro, N., Kadomatsu, K., 2012. CD44 expression in astrocytes and microglia is associated with ALS progression in a mouse model. Neurosci. Lett. 520, 115–120. https://doi.org/10.1016/j.neulet.2012.05.048.

McCauley, M.E., Baloh, R.H., 2018. Inflammation in ALS/FTD pathogenesis. Acta Neuropathol. https://doi.org/10.1007/s00401-018-1933-9.

Mishra, M., Paunesku, T., Woloschak, G.E., Siddique, T., Zhu, L.J., Lin, S., Greco, K., Bigio, E.H., 2007. Gene expression analysis of frontotemporal lobar degeneration of the motor neuron disease type with ubiquitinated inclusions. Acta Neuropathol. 114, 81–94. https://doi.org/10.1007/s00401-007-0240-7.

Morisaki, Y., Niikura, M., Watanabe, M., Onishi, K., Tanabe, S., Moriwaki, Y., Okuda, T., Ohara, S., Murayama, S., Takao, M., Uchida, S., Yamanaka, K., Misawa, H., 2016. Selective expression of osteopontin in ALS-resistant motor neurons is a critical determinant of late phase neurodegeneration mediated by matrix metalloproteinase-9. Sci. Rep. 6, 27354. https://doi.org/10.1038/srep27354.

Narain, P., Pandey, A., Gupta, S., Gomes, J., Bhatia, R., Vivekanandan, P., 2018. Targeted next-generation sequencing reveals novel and rare variants in Indian patients with amyotrophic lateral sclerosis. Neurobiol. Aging 71 265.e9-265.e14.

Novarino, G., Fabrizi, C., Tonini, R., Denti, M.A., Malchiodi-Albedi, F., Lauro, G.M., Sacchetti, B., Paradisi, S., Ferroni, A., Curmi, P.M., Breit, S.N., Mazzanti, M., 2004. Involvement of the intracellular ion channel CLIC1 in microglia-mediated beta-amyloid-induced neurotoxicity. J. Neurosci. 24, 5322–5330. https://doi.org/10.1523/JNEUROSCI.1170-04.2004.

Ohkawa, Y., Ohmi, Y., Tajima, O., Yamauchi, Y., Furukawa, K., Furukawa, K., 2011. Wisp2/CCN5 up-regulated in the central nervous system of GM3-only mice facilitates neurite formation in Neuro2a cells via integrin-Akt signaling. Biochem. Biophys. Res. Commun. 411, 483–489. https://doi.org/10.1016/j.bbrc.2011.06.118.

Parkinson, N., Ince, P.G., Smith, M.O., Highley, R., Skibinski, G., Andersen, P.M., Morrison, K.E., Pall, H.S., Hardiman, O., Collinge, J., Shaw, P.J., Fisher, E.M., Study M.R.C.P., Consortium F.R., 2006. ALS phenotypes with mutations in CHMP2B (charged multivesicular body protein 2B). Neurology 67, 1074–1077. https://doi.org/10.1212/01.wnl.0000231510.89311.8b.

Patel, A., Rees, S.D., Kelly, M.A., Bain, S.C., Barnett, A.H., Thalitaya, D., Prasher, V.P., 2011. Association of variants within APOE, SORL1, RUNX1, BACE1 and ALDH18A1 with dementia in Alzheimer's disease in subjects with Down syndrome. Neurosci. Lett. 487, 144–148. https://doi.org/10.1016/j.neulet.2010.10.010.

Peterson, L.J., Flood, P.M., 2012. Oxidative stress and microglial cells in Parkinson's disease. Mediat. Inflamm. 2012, 401264. https://doi.org/10.1155/2012/401264.

Phukan, J., Elamin, M., Bede, P., Jordan, N., Gallagher, L., Byrne, S., Lynch, C., Pender, N., Hardiman, O., 2012. The syndrome of cognitive impairment in amyotrophic lateral sclerosis: a population-based study. J. Neurol. Neurosurg. Psychiatry 83, 102–108. https://doi.org/10.1136/jnnp-2011-300188.

Prado, L.G.R., Rocha, N.P., de Souza, L.C., Bicalho, I.C.S., Gomez, R.S., Vidigal-Lopes, M., Braz, N.F.T., Vieira, E.L.M., Teixeira, A.L., 2018. Longitudinal assessment of clinical and inflammatory markers in patients with amyotrophic lateral sclerosis. J. Neurol. Sci. 394, 69–74. https://doi.org/10.1016/j.jns.2018.08.033.

Pramatarova, A., Laganiere, J., Roussel, J., Brisebois, K., Rouleau, G.A., 2001. Neuron-specific expression of mutant superoxide dismutase 1 in transgenic mice does not lead to motor impairment. J. Neurosci. 21, 3369–3374. https://doi.org/10.1523/JNEUROSCI.21-10-03369.2001.

Pressman, P.S., Miller, B.L., 2014. Diagnosis and management of behavioral variant frontotemporal dementia. Biol. Psychiatry 75, 574–581. https://doi.org/10.1016/j.biopsych.2013.11.006.

Qian, K., Huang, H., Peterson, A., Hu, B., Maragakis, N.J., Ming, G.L., Chen, H., Zhang, S.C., 2017. Sporadic ALS astrocytes induce neuronal degeneration in vivo. Stem Cell Rep. 8, 843–855. https://doi.org/10.1016/j.stemcr.2017.03.003.

Ratnavalli, E., Brayne, C., Dawson, K., Hodges, J.R., 2002. The prevalence of frontotemporal dementia. Neurology 58, 1615–1621. https://doi.org/10.1212/WNL.58.11.1615.

Rho, J.M., Szot, P., Tempel, B.L., Schwartzkroin, P.A., 1999. Developmental seizure susceptibility of kv1.1 potassium channel knockout mice. Dev. Neurosci. 21, 320–327. https://doi.org/10.1159/000017381.

Ripps, M.E., Huntley, G.W., Hof, P.R., Morrison, J.H., Gordon, J.W., 1995. Transgenic mice expressing an altered murine superoxide dismutase gene provide an animal model of amyotrophic lateral sclerosis. Proc. Natl. Acad. Sci. U. S. A. 92, 689–693.

Roos, P., von Essen, M.R., Nielsen, T.T., Johannsen, P., Stokholm, J., Bie, A.S., Waldemar, G., Simonsen, A.H., Heslegrave, A., Zetterberg, H., Consortium, F.R., Sellebjerg, F., Nielsen, J.E., 2018. Inflammatory markers of CHMP2B-mediated frontotemporal dementia. J. Neuroimmunol. 324, 136–142. https://doi.org/10.1016/j.jneuroim.2018.08.009.

Schmitt, F., Hussain, G., Dupuis, L., Loeffler, J.P., Henriques, A., 2014. A plural role for lipids in motor neuron diseases: energy, signaling and structure. Front. Cell. Neurosci. 8, 25. https://doi.org/10.3389/fncel.2014.00025.

Schulthess, J., Meresse, B., Ramiro-Puig, E., Montcuquet, N., Darche, S., Begue, B., Ruemmele, F., Combadiere, C., Di Santo, J.P., Buzoni-Gatel, D., Cerf-Bensussan, N., 2012. Interleukin-15-dependent NKp46+ innate lymphoid cells control intestinal inflammation by recruiting inflammatory monocytes. Immunity 37, 108–121. https://doi.org/10.1016/j.immuni.2012.05.013.

Sevastou, I., Pryce, G., Baker, D., Selwood, D.L., 2016. Characterisation of transcriptional changes in the spinal cord of the progressive experimental autoimmune encephalomyelitis Biozzi ABH mouse model by RNA sequencing. PLoS One 11, e0157754. https://doi.org/10.1371/journal.pone.0157754.

Skibinski, G., Parkinson, N.J., Brown, J.M., Chakrabarti, L., Lloyd, S.L., Hummerich, H., Nielsen, J.E., Hodges, J.R., Spillantini, M.G., Thusgaard, T., Brandner, S., Brun, A., Rossor, M.N., Gade, A., Johannsen, P., Sorensen, S.A., Gydesen, S., Fisher, E.M., Collinge, J., 2005. Mutations in the endosomal ESCRTIII-complex subunit CHMP2B in frontotemporal dementia. Nat. Genet. 37, 806–808. https://doi.org/10.1038/ng1609.

Sun, S., Sun, Y., Ling, S.C., Ferraiuolo, L., McAlonis-Downes, M., Zou, Y., Drenner, K., Wang, Y., Ditsworth, D., Tokunaga, S., Kopelevich, A., Kaspar, B.K., Lagier-Tourenne,

C., Cleveland, D.W., 2015. Translational profiling identifies a cascade of damage initiated in motor neurons and spreading to glia in mutant SOD1-mediated ALS. Proc. Natl. Acad. Sci. U. S. A. 112, E6993–E7002. https://doi.org/10.1073/pnas.1520639112.

Tortarolo, M., Vallarola, A., Lidonnici, D., Battaglia, E., Gensano, F., Spaltro, G., Fiordaliso, F., Corbelli, A., Garetto, S., Martini, E., Pasetto, L., Kallikourdis, M., Bonetto, V., Bendotti, C., 2015. Lack of TNF-alpha receptor type 2 protects motor neurons in a cellular model of amyotrophic lateral sclerosis and in mutant SOD1 mice but does not affect disease progression. J. Neurochem. 135, 109–124. https://doi.org/10.1111/jnc.13154.

Urwin, H., Ghazi-Noori, S., Collinge, J., Isaacs, A., 2009. The role of CHMP2B in frontotemporal dementia. Biochem. Soc. Trans. 37, 208–212. https://doi.org/10.1042/BST0370208.

van Blitterswijk, M., Vlam, L., van Es, M.A., van der Pol, W.L., Hennekam, E.A., Dooijes, D., Schelhaas, H.J., van der Kooi, A.J., de Visser, M., Veldink, J.H., van den Berg, L.H., 2012. Genetic overlap between apparently sporadic motor neuron diseases. PLoS One 7 (11), e48983. https://doi.org/10.1371/journal.pone.0048983.

van der Zee, J., Urwin, H., Engelborghs, S., Bruyland, M., Vandenberghe, R., Dermaut, B., De Pooter, T., Peeters, K., Santens, P., De Deyn, P.P., Fisher, E.M., Collinge, J., Isaacs, A.M., Van Broeckhoven, C., 2008. CHMP2B C-truncating mutations in frontotemporal lobar degeneration are associated with an aberrant endosomal phenotype in vitro. Hum. Mol. Genet. 17, 313–322. https://doi.org/10.1093/hmg/ddm309.

Vernay, A., Therreau, L., Blot, B., Risson, V., Dirrig-Grosch, S., Waegaert, R., Lequeu, T., Sellal, F., Schaeffer, L., Sadoul, R., Loeffler, J.P., Rene, F., 2016. A transgenic mouse expressing CHMP2Bintron5 mutant in neurons develops histological and behavioural features of amyotrophic lateral sclerosis and frontotemporal dementia. Hum. Mol. Genet. 25, 3341–3360. https://doi.org/10.1093/hmg/ddw182.

Vlug, A.S., Teuling, E., Haasdijk, E.D., French, P., Hoogenraad, C.C., Jaarsma, D., 2005. ATF3 expression precedes death of spinal motoneurons in amyotrophic lateral sclerosis-SOD1 transgenic mice and correlates with c-Jun phosphorylation, CHOP expression, somato-dendritic ubiquitination and Golgi fragmentation. Eur. J. Neurosci. 22, 1881–1894. https://doi.org/10.1111/j.1460-9568.2005.04389.x.

Vucic, S., Kiernan, M.C., 2006. Novel threshold tracking techniques suggest that cortical hyperexcitability is an early feature of motor neuron disease. Brain 129, 2436–2446. https://doi.org/10.1093/brain/awl172.

Wahrle, S.E., Jiang, H., Parsadanian, M., Legleiter, J., Han, X., Fryer, J.D., Kowalewski, T., Holtzman, D.M., 2004. ABCA1 is required for normal central nervous system ApoE levels and for lipidation of astrocyte-secreted apoE. J. Biol. Chem. 279, 40987–40993. https://doi.org/10.1074/jbc.M407963200.

Wakade, C., Chong, R., Bradley, E., Thomas, B., Morgan, J., 2014. Upregulation of GPR109A in Parkinson's disease. PLoS One 9, e109818. https://doi.org/10.1371/journal.pone.0109818.

Yamamoto, T., Murayama, S., Takao, M., Isa, T., Higo, N., 2017. Expression of secreted phosphoprotein 1 (osteopontin) in human sensorimotor cortex and spinal cord: changes in patients with amyotrophic lateral sclerosis. Brain Res. 1655, 168–175. https://doi.org/10.1016/j.brainres.2016.10.030.

Yan, J., Xu, Y., Zhang, L., Zhao, H., Jin, L., Liu, W.G., Weng, L.H., Li, Z.H., Chen, L., 2016. Increased expressions of plasma galectin-3 in patients with amyotrophic lateral sclerosis. Chin. Med. J. 129, 2797–2803. https://doi.org/10.4103/0366-6999.194656.

Yang, B., Oo, T.N., Rizzo, V., 2006. Lipid rafts mediate H2O2 prosurvival effects in cultured endothelial cells. FASEB J. 20, 1501–1503. https://doi.org/10.1096/fj.05-5359fje.

Ylikallio, E., Konovalova, S., Dhungana, Y., Hilander, T., Junna, N., Partanen, J.V., Toppila, J.P., Auranen, M., Tyynismaa, H., 2015. Truncated HSPB1 causes axonal neuropathy and impairs tolerance to unfolded protein stress. BBA Clin. 3, 233–242. https://doi.org/10.1016/j.bbacli.2015.03.002.

Zhang, Y., Schmid, B., Nikolaisen, N.K., Rasmussen, M.A., Aldana, B.I., Agger, M., Calloe, K., Stummann, T.C., Larsen, H.M., Nielsen, T.T., Huang, J., Xu, F., Liu, X., Bolund, L., Meyer, M., Bak, L.K., Waagepetersen, H.S., Luo, Y., Nielsen, J.E., Consortium, F.R., Holst, B., Clausen, C., Hyttel, P., Freude, K.K., 2017. Patient iPSC-derived neurons for disease modeling of frontotemporal dementia with mutation in CHMP2B. Stem Cell Reports. 8, 648–658. https://doi.org/10.1016/j.stemcr.2017.01.012.

Zoghbi, H.Y., Gage, F.H., Choi, D.W., 2000. Neurobiology of disease. Curr. Opin. Neurobiol. 10, 655–660. https://doi.org/10.1016/S0959-4388(00)00135-5.